M.Tech. (Computational Design)

[Nishant Srivastava]

2019

VELOCITY ENHANCEMENT OF HYDROKINETIC TURBINE OPERATION IN OPEN CHANNELS USING A MUTLI AEROFOIL DIFFUSER

A PROJECT REPORT

SUBMITTED IN PARTIAL FULFILLMENT OF THE REQUIREMENTS

FOR THE AWARD OF THE DEGREE

OF

MASTER OF TECHNOLOGY

IN

COMPUTATIONAL DESIGN

Submitted by:

NISHANT SRIVASTAVA

(2K17/CDN/02)

Under the supervision of

PROF. A.K. AGRAWAL

DEPARTMENT OF MECHANICAL ENGINEERING

DELHI TECHNOLOGICAL UNIVERSITY

(Formerly Delhi College of Engineering)

Bawana Road, Delhi-110042

JULY, 2019

DEPARTMENT OF MECHANICAL ENGINEERING

DELHI TECHNOLOGICAL UNIVERSITY

(Formerly Delhi College of Engineering)

Bawana Road, New Delhi -110042

CANDIDATE'S DECLARATION

I, Nishant Srivastava, Roll No. 2K17/CDN/02, student of M.Tech. (Computational Design), hereby declare that the project dissertation titled "Velocity enhancement of hydrokinetic turbine operation in open channels using a mutli aerofoil diffuser" which is submitted by me to the Department of Mechanical Engineering, Delhi Technological University, Delhi in partial fulfillment of the requirement for the award of the degree of Master of Technology, is original and not copied from any source without proper citation. This work has not previously formed the basis for the award of any degree, diploma associateship, fellowship or other similar title or recognition.

Place: New Delhi **Nishant Srivastava**

Date: **(2K17/CDN/02)**

DEPARTMENT OF MECHANICAL ENGINEERING,

DELHI TECHNOLOGICAL UNIVERSITY

(Formerly Delhi College of Engineering)

Bawana Road, New Delhi -110042

CERTIFICATE

I hereby certify that the Project Dissertation titled "Velocity enhancement of hydrokinetic turbine operation in open channels using a mutli aerofoil diffuser" which was submitted by Nishant Srivastava, Roll No.- 2K17/CDN/02, Department of Mechanical Engineering, Delhi Technological University, New Delhi in the partial fulfillment of the requirement for the award of the degree of Master of Technology, is a record of the project carried out by the student under my supervision. To the best of my knowledge this work has not been submitted in part or full for any Degree or Diploma in this University or elsewhere.

Place: Delhi

Date:

PROF. A.K. AGRAWAL

SUPERVISOR

Professor

Department of Mechanical Engineering

Delhi Technological University

ACKNOWLEDGEMENT

"It is not possible to prepare a report without the assistance & encouragement of other people. This one is certainly no exception. "

On the very outset of this report, I would like to extend my sincere & heartfelt obligation towards all the personages who have helped me in this endeavor. Without their active guidance, help, cooperation & encouragement, I would not have made headway in the project.

I am ineffably indebted to **Dr. Vipin**, HOD-Department of Mechanical Engineering for taking pain-staking efforts & **Prof. Atul Kumar Agrawal** for his conscientious guidance and encouragement to accomplish this assignment.

I extend my heartiest gratitude to DTU for giving me this opportunity. I also acknowledge with a deep sense of reverence, my gratitude towards my parents and member of my family, who has always supported me morally as well as economically.

At last but not least gratitude goes to all of my friends who directly or indirectly helped me to complete this report. Any omission in this brief acknowledgement does not mean lack of gratitude.

ABSTRACT

Indian states are full of canals and waterways used for irrigation and as water transport in different parts of the country. Installing low-cost hydrokinetic turbines in these canals can prove highly beneficial and would reduce the operational load on the conventional power generation units.

However, there is a limitation on the maximum energy that can be extracted from the flowing stream by these turbines. Thus, diffusers or ducts are modeled around these turbines to increase the power output of these turbines. The axial hydrokinetic turbines are the most commonly used turbines for extracting the energy of a flowing water current, river, ocean or tides.

This paper focuses on the development of a multi aerofoil diffuser profile that can increase the power output of these axial hydrokinetic turbines. This is done by using high lift aerofoil geometries to model the diffuser which leads to a velocity enhancement of the flow around the turbine. The effect of the variation of different diffuser angles of the secondary diffuser on the flow velocity is considered. Also, the pressure distributions along the exit area of the turbine are also studied.

Development of such efficient geometries of diffuser can lead to widespread application of this technology and thus provide renewable power to the masses at lesser costs.

CONTENTS

LIST OF FIGURES

LIST OF TABLES

LIST OF SYMBOLS

Symbol	Interpretation
P	Turbine output power
P	Fluid density
A	Area swept by the rotor blade
V_0	Velocity of the free stream
C_p	Coefficient of power
η	Drive train efficiency
Θ	Angle of diffuser
C_{Pi}	Ideal power coefficient
C_{PR}	Duct pressure recovery coefficient
C_{P4}	Base pressure coefficient
ΔP_{23}	Pressure drop across the throat area
C_{Pe}	Shroud exit pressure coefficient
ε	Velocity ratio
λ	Area ratio
η_D	Efficiency of the diffuser
r	Relative power coefficient
C_T	Turbine Load Factor
v_t	Velocity at throat

P_e	Pressure at exit
P_0	Pressure at upstream conditions
A_e	Area at the exit of diifuser
A_t	Area at the throat of the diffuser
x,y,z	Coordinate axes
1,2,3,4	Position of stations in a DAWT

CHAPTER 1: INTRODUCTION

Hydrokinetic energy conversion has been an area of immense interest over the last few decades with extensive research going on in the development and widespread application of such systems. As the whole world is shifting from the use of conventional energy generation methods towards the use of renewable energy, the possibility of capturing the energy in tidal currents in the sea, flowing river streams, and man-made channels has proven to be quite an interesting one.

The hydrokinetic energy conversion process aims at utilizing the kinetic energy of the water flowing in tidal currents, river streams and artificial waterways to generate mechanical power which can be further converted into electrical power by the use of a generator. Different types of turbine systems e.g. Horizontal (axial), Vertical, or Cross-flow or non-turbine systems can be utilized to extract this power from the water.

With the ever-increasing energy demands all across the globe, and the inability of the conventional energy generation methods to keep up with these demands in a manner that doesn't cause damage to the environment, using such renewable energy systems has become quite paramount in nature.

1.1 HYDROKINETIC ENERGY CONVERSION METHODS

Most hydrokinetic conversion processes employ the use of turbine type systems to extract the energy from the flowing water, however some non-turbine methods are also being researched for the same.

1.2 TURBINE SYSTEMS

These can be further classified into following types:

- Horizontal-axis turbines: This arrangement has the axis of the turbine rotor parallel to the flowing water stream. Generally utilizing various High lift airfoil geometries for the construction of their blades, these turbines are one of the most commonly used setups for extracting energy from the water.
- Vertical-axis turbines: In this arrangement, the axis of the turbine rotor is placed vertical to the direction of the flowing water stream e.g Darrieus, Savonius turbines.

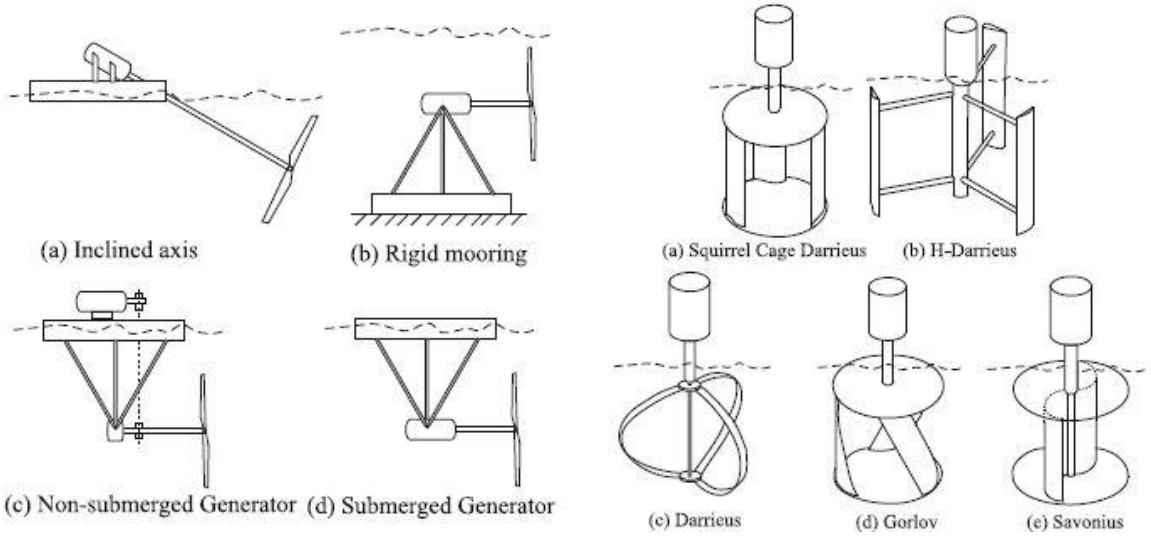

Fig. 1.1 Types of hydrokinetic turbines [8]

- Cross flow turbine: In this arrangement, the turbine rotor axis is parallel to the surface of water but orthogonal to the direction of the flowing water stream.
- Venturi: Water accelerated with the help of choke system is used to generate a pressure gradient which is used to drive the turbine system.
- Gravitational Vortex: A vertical-axis turbine is driven with the help of an artificially created vortex effect.

1.3 NON-TURBINE SYSTEMS

These employ various unconventional methods for capturing the hydrokinetic energy:

- Oscillating hydrofoil: It employs the vertical oscillation of hydrofoils to generate pressure in fluids for turbine operation.
- Piezoelectric: A sheet of a piezo-electric material is placed in the flowing water stream and electricity is generated due to the disturbances created on the material.
- - Flutter vane: Flutter (Hydro-elastic resonance) in the free-flowing water stream is used for the power generation.
- Vortex induced vibration: These employ vibrations resulting from the formation and shedding of vortices on the downstream portion of a bluff body placed in the stream.

1.4 DIFFUSER AUGMENTATION

Diffusers (or shrouds) are aerodynamic structures, commonly employed for the purpose of Power augmentation of hydrokinetic turbines. There are different types of diffusers configurations in active deployment while some are still in the developmental phase. They are generally intended to enhance the power output of the hydrokinetic turbine and optimize its performance by further accelerating the mass flow rate through the turbine. These also help in lowering the starting torque of the rotor and increasing its speed of rotation, and also protecting the marine life from the blades of the turbine. The development of improved analysis methods for fluid dynamics e.g. BEM (Blade Element Momentum) theory and CFD (Computational Fluid Dynamics) has led to a lot of research in the development of such diffuser models that can increase the performance of these turbines in an economical manner.

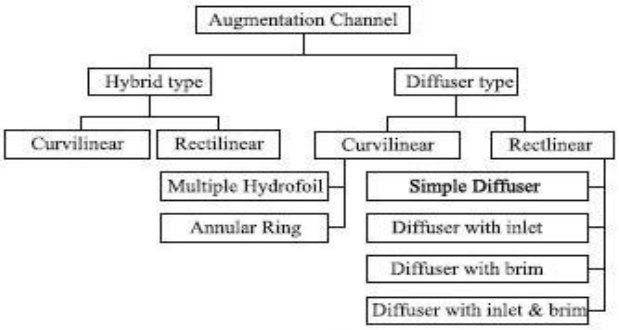

Fig. 1.2 Types of augmentation channels [8]

1.4.1 SIMPLE DIFFUSER

These diffusers generally involve a simple converging-diverging profile with the turbine positioned at the smallest cross-section, generally referred to as the throat. The profile of the diffuser can be rectilinear, curvilinear, or aerofoil in shape.

1.4.2 DIFFUSER WITH BRIM/FLANGE

Experiments were conducted to study the best design of the diffuser brim and flange technology diffuser increase the output to 2.6 times the ordinary turbine. With brim based yaw controlled technology bring about the position of the tribune according to the flow of the wind energy. With positive changes in design and compactness this appears to be of great success. This new design of diffuser is further studied and it shows the same results for bare turbine as well as flanged diffuser hydro kinetic turbines. Vortex structure rapidly deteriorates at exit for both bare turbine and flanged diffuser turbine.

1.4.3 MULTI-SLOT DIFFUSER

The use of multi slot diffuser is to allow the maximum passage of air intake. It reenergizes the inner boundary layer inside the diffuser using high lift aerofoil. It helps in creating a low value of velocity and pressure thus high air mass flow rate inside the diffuser. Using of one or more diffuser ring, subsequently increases the area and thus the mass flow rate. The length to diameter ratio of the diffuser reduces drastically by employing this method of multiple slot which makes the turbine more compact and light weight.

1.4.4 VORTICITY-BASED DIFFUSER

This method is used to lowering the fluid pressure and thus increasing the fluid differential across the diffuser. Although in reality achieving this type of condition is quiet typical unpredictable nature of fluid flow. Diffuser geometry with an area ratio of 4.4 and an angle of 16^{o} shows 60% less loses in total diffuser loses. In other cases when the area ratio of 2 and the various diffuser half angles of 2^{o}, 3.5^{o}, 5^{o} shows the overall increase in performance of about 25%.

1.4.5 MIXER-EJECTOR DIFFUSER

This diffuser aims at mixing the low velocity turbine exit fluid with the second stage high entering fluid. This method has increase the productivity of turbines by a factor of 2. It allows the use of single or multi ejector pin which to increase the Betz. Limit. For mixing streamwise vortices vortex generators and lobed mixers can be used.

1.4.6 ROTATING DIFFUSER

In these types of diffuser, diffuser can rotate horizontally along the axis of the turbine thus named rotating diffuser. The diffuser has an attachment along the exit end of the diffuser to fill the gap for entry to the turbine. The use of guide vanes and vortex generator are used to avert the air flow twisting. The rotor is made up of a wear resistant material (ABS acrylic) which is light in weight and is easy to maintain. This technology made the diffuser blade less susceptible to vibrations.

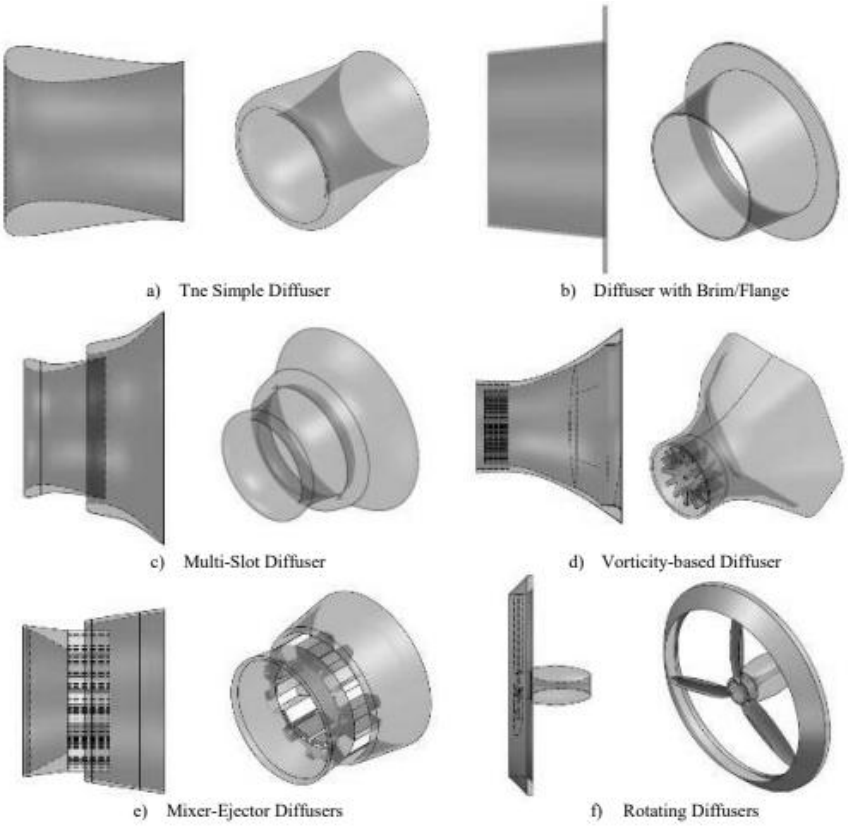

Fig. 1.3 Types of diffusers [24]

1.5 Power generation in a Hydrokinetic Turbine:

The minimum operable range of hydrokinetic turbine is around 2-4 knots, whereas the optimum range of current is the range of 5-7 knots. Since, the diameter of the rotor depends upon the level of water, adequate depth of water is also a crucial factor in determining the total energy. Thus, for axial hydrokinetic turbines, The turbine output power (P) can be represented as

:

$$\mathbf{P = (½)*\rho*A*Vo*Cp*\eta}$$

The output power similar to that in wind turbines which is a function of the fluid density (ρ) and area swept by the rotor blade ($A = \pi R^2$) where R is the radius of blade, velocity (V_1), the power coefficient (C_p) and drive train efficiency (η), which is considered 70%, a conservative value for a small turbine for electric generation. The theoretical limit of Cp, concluded by Bezt, is 0.593.

CHAPTER 2: LITERATURE REVIEW

The literature review of the project consists the title, research work, parameter and results of the different research papers.

Lilley G. M. et. al. [1] (1956) assessed the use of a Diffuser utilizing the existing 1D theory, by comparing the performance of 'un-shrouded windmills' to 'ducted windmills'. Based on the 1D theory, a 65% increase in maximum power was attained by using a duct with an Area Ratio of 3.5 and a 15% pressure loss compared to a conventional system. The analysis was however based on rough geometries.

Igra O. et. al. [2] (1976) performed an investigation on different techniques to reduce the large length-diameter ratio for a given Area ratio required in a Diffuser without affecting performance. In the experiment, blowing and bleeding effects in a Straight wall diffuser with a series of drilled-in ports at the rear end of the shroud were investigated and the effects of using an aerofoil shaped axi-symmetric flap (NACA4412) and a flat plate ring-flap was studied and compared. It was concluded that bleeding through all ports didn't enhance flow separation but introduced the system to more turbulence. While blowing through some ports in the higher-pressure region of the Diffuser was able to increase output power by 20%. The aerofoil ring-flaps was found to be more effective than the flat plate ring flap, as the former increased power up to 65% .

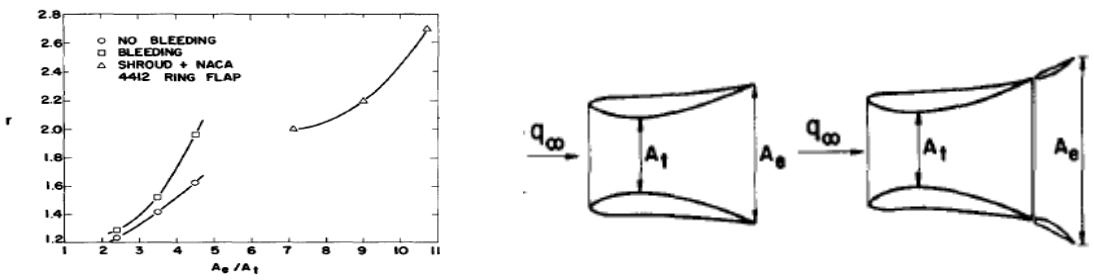

Fig. 2.1. Power ratio vs. area ratio curves for different setups [2]

Foreman K. M et.al. [3] (1977) investigated of models of two diffuser design concepts for the development of small size and cost-effective diffuser configurations. One approach uses the injection of energetic external wind to prevent boundary layer separation along the internal profile of the diffuser. Another method uses high lift aerofoil contours for the diffuser wall shape. Model tests have demonstrated significant power augmentation capabilities for DAWT, approaching a factor of 2.

Ponta F. et. al. [4] (1999) worked on the development of a `Self-Regulated Vertical-Axis Hydroturbine' with a channelling device which consists of two pontoons set side-by side, with a vertical axis Darrieus rotor set between them.

A set of experiments were performed in a Hydrodynamic Test Canal for the selection of an optimum hydrodynamic profile for the channelling device based on Flow speed Flow depth, Flow lines visualization and Output Power measurement. Out of all the profiles tested (profileA0A1, D1A1, D1B3, E1A3, E1C3,E1A6), the profile E1A6 presents the most interesting combination of characteristics: high velocity gain at low and medium current speeds of the river and an adequate attenuation at high river flow speeds.

For a nominal Output power of 5-kW, the performance of the classic WCT decays notably at low speeds whereas it is not case for the E1A6-WCT because of the self-regulation effect produced by the channelling device.

Upon observing the flow speed in the rotor insertion zone as a function of the river current speed, from the theoretical and experimental bases, it was found that the values are in agreement for subcritical and supercritical flow but noticeable difference are there in the transition zone as might be expected since this zone is at the edge of the validity range of every theoretical model.

Setoguchi T. et. al. [5] (2004) The main objective of the study was to study the effect of the Brim height and the Outside body shape on the diffuser performance.

Experimental investigation of the performance of a two-way diffuser system in air with different outside body shapes (base type, bulge type, straight type) with three kinds of brim

heights (H=0,H=D, H=2D, H= height of the brim, D= tip diameter of the turbine blades)was done in a low speed wind tunnel setup.

The Static pressure distributions as well as the z-Directional velocity distributions on the center-axis of each type of diffuser for each brim height were experimentally measured to observe the effects of the brim height and the outside body shape on the performance of the diffuser system.

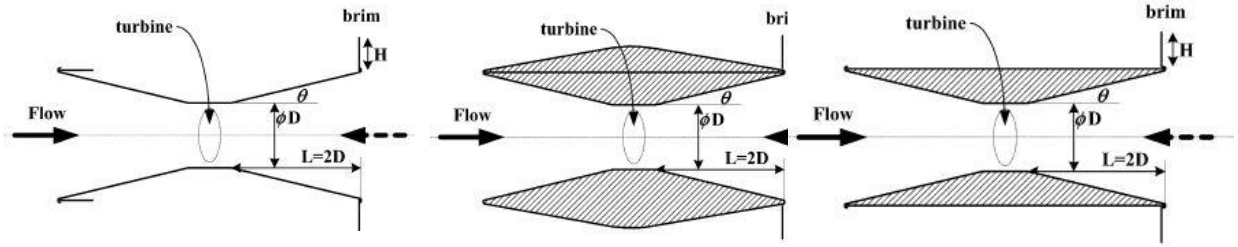

Fig.2.2 Outline of (a) 'base type', (b) 'bulge type', (c) 'straight type' diffusers [5]

In this experiment, the best performance is obtained in the case of the 'straight type' diffuser with a brim of H/D= 2. In this case, the flow velocity through the turbine area is accelerated up to 1.3 times the main flow velocity. The effect of the brim on the diffuser performance with any of the outside body shape is confirmed. It gets maximized when the external flow along the outside body of the diffuser is controlled by the use of the outside body shape.

Other outside body shapes could have been considered and their effect on the Diffuser performance can be studied.

David L. F. Gaden et. al. [6] (2006) The objective of the study was to attain cost-effective distributed power generation by increasing Power Density of Kinetic Turbines with the help of a shroud-type setup for water current turbines.

ANSYS CFX-5.7, commercial CFD simulation software was used to perform the calculations. The fluid was modelled as incompressible, under steady-state conditions, with a k-ε turbulence model. A numerical study of diffuser area ratio and diffuser angle was done to find the optimum values for the diffuser design.

The optimum diameter ratio was found to be a diffuser with a 3.0m outlet diameter and an angle of 20° to the stream-wise direction. Simulations presented showed the power

increases by a factor of 3.1 with a drag increase factor of 3.9. However, experimentation has not been performed to validate the numerical simulations presented here. In this paper, the diffuser is modelled as a simple cylindrical wall with a conical section. It is expected that a more streamlined design will perform better, such as a hydrofoil shape. The possibility of development of a multi-section slotted diffuser can also be considered.

Ponta F. L. et. al. [7] (2007) The paper studies various trends in marine-current energy and the different technological challenges to the development of marine current turbines. Further, a diffuser-augmented floating hydrokinetic turbine and its design and optimization are considered. Placing all the mechanical components in a protected casing helps in protecting the bearings and other components from the leakage of pressurized sea water. This layout also presents the advantage that all the mechanical and electrical gear may be quite accessible to easy on-deck maintenance or could even be completely replaced.
There still remains to be considered the question of rotor's materials and construction techniques. Various materials ranging from Steel blades to glass fiber with carbon-fiber reinforced main Spars can be considered.

Khan M. J. et. al. [8] (2009) Review of various pre-existing and upcoming Hydrokinetic energy conversion systems is done which covers Turbine systems (Horizontal, Vertical, Crossflow, Venturi, Gravitational vortex etc.) as well as Non-turbine systems (Flutter vanes, piezoelectric systems, Vortex induced vibration, Oscillating hydrofoil, Sails).
Various features like Design features (size and placement of the turbine, directionality of the flow) and Operational features (Flow characteristics, water density, control, resource prediction) and End-use applications is done for Tidal as well as River applications.
Out of the 76 different devices and schemes that were analyzed it was found that Axial and Vertical Turbine systems were found to be the most widely used (43% and 33% respectively). Further, various aspects of these turbine systems were discussed e.g.
Rotor configurations for HAHT (Inclined/Straight axis, Solid/ Buoyant mooring, Submerged/Non-submerged Generator) and VAHT (Squirrel Cage Darrieus, Darrieus (Straight/Curved Blade), Gorlov, Savonius etc.)

Duct Augmentation- Hybrid-type(Curvilinear/ Rectilinear) and Diffuser-type (Curvilinear (Multiple Hydrofoil/ Annular Ring) or Rectilinear (Simple Diffuser/ Diffuser with inlet/ diffuser with brim/ diffuser with inlet and brim)

Rotor placement options (BSM – Bottom Structure Mounted (Fixed), FSM – Floating Structure Mounted (Buoyant), and NSM – Near-surface Structure Mounted (Fixed).

Apart from the River and Tidal energy conversion, other resources (like man-made canals, irrigation channels, and industrial outflows) also have the potential for deploying this technology. Out of all the arrangements used, axial and vertical turbine systems are the most preferred one for practical applications.

Duct Augmentation for Vertical turbines is preferred than for axial turbines due to the design asymmetry and structural vulnerability imposed because of the fact that the ducts for HAHT mostly take conical shapes whereas the channels are of rectangular cross-section in case of VAHT. Axial turbines are mostly being considered for placement at the bottom of a channel, whereas vertical turbines are being designed for either floating or near-surface mounting arrangements.

David L.F. Gaden et. al. [9] (2009) This numerical study investigates the use of diffusers to enhance the performance and viability of kinetic hydro turbines.

ANSYS CFX, commercially available finite volume CFD software is used to perform the numerical simulations. The Momentum source modelling strategy is used to represent the turbine, by removing the geometry of the turbine and applying a momentum source evenly throughout the region where the turbine would’ve been, causing the fluid to lose the energy normally extracted by the turbine.The relationship between the diffuser size and its effect on overall performance is evaluated by varying the area ratio and the diffuser angle as well, and power output and drag coefficients are calculated to determine their optimum value.

The power output initially increases linearly with the area ratio, rising from 16.4 kW for no diffuser to 38.7 kW for an area ratio of 1.266. That is an increase by a factor 2.36 where the diffuser radius grew by only 12.5%.

Power output is greatest at shallow diffuser angles of 20^{o} to 30^{o}, and drops off at angles outside of this. The optimized diffuser angle of 20^{o} most closely follows the streamlines as they exit the diffuser.

The shroud and diffuser modelled in this study have a simple cylindrical and conical geometry. Further benefit is expected using curved profiles.

Ohya Y. et. al. [10] (2010): Development of a new wind turbine system that consists of a diffuser shroud with a broad-ring brim at the exit periphery.

Two type of hollow structure models (a nozzle and a diffuser with a L/D= 7.7) and a short diffuser with a brim were tested in a wind tunnel with an open-type test section. Wind velocity (u) and static pressure(p) distributions along the central axis of the hollow-structure model were obtained with a I-type hot-wire and a static-pressure tube. The smoke-wire technique was employed for the flow visualization experiment.

Further , an output performance test for the brimmed diffuser with different outlet brim profiles (Aii, Bii, Cii and Sii type) is performed with a torque transducer connected to the wind turbine and in the rear of it.

Significant increase in the output power of a micro-scale wind turbine was obtained.

With a relatively long diffuser (Lt = 1.47D), a remarkable increase in the output power of approximately 4–5-times that of a conventional wind turbine is achieved. This is because a low-pressure region due to a strong vortex formation behind the broad brim draws more mass flow to the wind turbine inside the diffuser.

The possibility of a development of such a shrouded setup for a hydrokinetic turbine can be considered.

Kirke B. K. et. al. [11] (2011) This paper summarises the findings of a series of tests on several Darrieus type cross flow hydrokinetic turbines.

HKTs with fixed and variable pitch straight blades, fixed helical blades, with and without a slatted diffuser, by mounting each turbine in front of a barge and motoring through still water at speeds ranging from less than 1 m/s up to 5 m/s. The diffuser increased the power output by a factor of 3 in one configuration but considerably less in others.

The maximum coefficient of performance Cp of the fixed pitch straight blade and helical turbines without a diffuser ranged from about 0.25 at 1.5 m/s down to less than 0.1 at 5 m/s, while Cp for those with a diffuser ranged from about 0.45 down to about 0.3. Fixed blade turbines, both straight and helical, exhibited low starting torque, while variable pitch

turbines started easily. Considerable differences in Cp were observed for the same turbine configuration at different speeds. The turbine with fixed pitch, straight blades was found to shake violently due to cyclical hydrodynamic forces on blades, while the helical and variable pitch turbines did not shake excessively.
These findings suggest that variable pitch cross flow HKTs should be further investigated.

Malipeddi A. R. et. al. [12] (2012) to develop a new duct with the purpose of improving the performance of a straight-bladed Darrieus hydro-turbine and to retain the simple design and fabrication procedure while reducing the disadvantages

A new duct is developed, for a given turbine design, that reduces the variation in torque over a cycle by appropriately directing the flow upstream and downstream the turbine while increasing power conversion.
At the operating point, which is at a tip-speed ratio of 2, use of a duct reduces the torque ripple by a factor of 4.15 and the power coefficient (Cp) is increased to 0.63 from 0.40. By choosing the position of the turbine in the duct appropriately, it is shown that the torque ripple may be reduced by a factor of 6.37, at the expense of the power coefficient. And, a maximum Cp ¼ 0.644 is observed when the turbine center coincided with the throat of the duct. Similarly,the effect of varying other parameters such as the convergence angle of the duct and its external shape on the performance of the turbine are studied through numerical simulation.
It is observed that the maximum power coefficient and lowest torque ripple are obtained at the same value of duct half angle, equal to 27^{o}. The duct with straight external shape is observed to have best performance with a peak power coefficient of 0.72, while the convex external shape has a peak of only 0.51. The external shape is observed to have a negligible effect of the torque ripple factor.
These findings suggest that variable pitch cross flow HKTs should be further investigated.

Chime A. H. [13] (2013): To find the maximum power that can be extracted from a HAHT (Horizontal axis Hydrokinetic Turbine) utilizing an open channel flow.
The methods used included: 1-D modeling using conservation of mass, linear momentum and energy equations, 3-D CFD modeling (Volume of Fluid model with Open Channel

Flow Boundary Conditions). Turbines were modeled using: Actuator Disc Model and Virtual Blade Model.Power generation vs. flow control was also measured.

A theoretical method uses one-dimensional control volume analysis to compute the maximum power that an ideal rotor can extract from the flow as useful power and as wake mixing loss at a given Froude number and blockage ratios.

Effect of Channel Constriction on Water Depth was also observed at different channel width (16m, 19m ,21m) and Blockage ratios (0.48, 0.40, 0.36) and Effect of Channel Constriction on Power Generation was also studied with 3 Turbines having 4 m diameterwith stream conditions (Flow rate= 130 m^3/s,) and Froude number=0.18-0.24

Three-dimensional Actuator Disc Model (ADM) developed in the Computational Fluid Dynamic (CFD) code ANSYS Fluent.This model uses a porous media to represent the HAHTs and Reynolds-Average Navier-Stokes (RANS) equations along with the Volume of Fluid (VoF) model to solve for the flow field and track the free surface.

Both 1D theory and 3D CFD show a 2% drop in water depth for the 21m case, and a 4% drop for the 16 m case.

The Virtual Blade Model (VBM), which uses Blade Element Theory (BET) to consider geometry of the blades and operating conditions such as the Tip Speed Ratio (TSR) and blade pitch angle. This method is used to optimize the turbine geometry for maximum power and to find operating limits to avoid blade cavitation.

From the Actuator Disk Model, It was found that the power extracted increases as blockage ratio increases. Wake recovery is faster for the flow when the blockage ratio is high compared to the flow at a lower blockage. This tendency appears to be caused by the higher velocity through and around the turbines when blockage ratio is high.

The literature lacks the experimental data for power extraction of HAHTs in high blockage ratio flows. Experiments must be performed using the designed turbine to validate the three-dimensional numerical and one-dimensional theoretical results

Luquet R. et. al. [14] (2013) This study has proved that the first configuration called ‘‘encased duct’’, brings a recovered power gain of 40%, comparatively with a single duct. This gain needs also to be put into perspective in the context of considering that the encased duct had a diameter that was twice that of the single duct. If the regular duct was

twice the diameter it will produce 4 times the power. So the main advantage of this configuration is not the power recovered but the huge velocity on the rotor which could enable the water turbine to product power at locations with very weak currents.
This configuration widens the places well-suited for water turbines. The second configuration, brings only a recovered power gain of 10%, incomparison with a single hull duct, for an equivalent overall dimension. The obtained gains, through this configuration, are low because it appears that the encased divergent does not reduce the separation but moves it from the duct trailing edge to the water turbine axis of symmetry.

Garcia E. [15](2014): It was observed from the simulation results that the efficiency improvement derived from the augmentation channel use expands the economic feasibility of our system to marine areas with lower current resources.
In particular, for type C augmentation channel the efficiency increase was 1.71 and for type I a maximum efficiency of 2.55 was achieved. For this last model a parametric variationanalysis was conducted. From the simulations we conclude that the best option for our prototype is based on the use of type I augmentation channel. Finally, a momentum source model was used to validate the system, taking into account the turbine effect. A simulation, modeling the whole blade geometry, was performed in order to validate the final design.

Aranake A. [16] (2014): In this work, the flow physics and performance of shrouded turbines is assessed by solving the Reynolds Averaged NaviersStokes equations supplemented with a transition model. Shroud geometries are evaluated for their augmentation of mass flow through the turbine. Initial assessments are performed using axisymmetric calculations of annular wings with high liftaerofoils as cross sections. The mass flow amplification factor is defined as a performance parameter and is found to increase nearly linearly with radial lift force. From a selection of considered aerofoils, the Selig S1223 high-lift aerofoil is found to best promote mass flow rate. Full three-dimensional
simulations of shrouded wind turbines are performed for selected shroud geometries. The results are compared to open turbine solutions. Augmentation ratios of up to 1.9 are

achieved. Peak augmentation occurs at the highest wind speed for which the flow over the blade stays attached. Flow fields are examined in detail and the following aspects are investigated: regions with flow separation, the development of velocity profiles, and the interaction between the turbine wake and shroud boundary layer. The sensitivity of the solutions to rotation rate is examined.

Mohammad S. [17] (2015) The objective of the paper was to study the Effect of shroud on the performance of horizontal axis Hydrokinetic turbines. Two shrouds (a convergent–divergent duct, and a straight wall duct) are fabricated and their effect on the performance of the model turbine is studied with the help of the experimental measurements performed in a water tunnel. Power and thrust coefficients of the model turbine with and without the shrouds investigated are obtained over the range of the power curve.

The shroud increases power of the turbine to some extent while the diffuser shows the most effectiveness. Maximum CP is 0.33, 0.38, and 0.40 for the bare turbine at flow speeds of 0.7, 0.9, and 1.1m/s, respectively. Maximum power coefficients increase to 0.50, 0.54, and 0.55 respectively.

An extended blade can substitute for a smaller blade with diffuser and generates the same power, which could be considered as a superior choice for the industry. However, a smaller shrouded blade can be a better choice for low speed flow sites.

Cresswell N. W. [18] (2015) The yaw effects on a diffuser- augmented turbine with quantification of blockage corrections and to study the wake recovery characteristics of these devices were examined. The testing of the Diffuser-augmented turbine was done in a 3/4 open-jet, open-return wind tunnel. The blades of the turbine were developed using NACA 63818 profile with the section's lift and drag performance obtained through CFD analysis done using ANSYS Fluent with the Transition SST turbulence model.The diffuser geometry was developed by utilising an optimization based around CFD, with a Kriging surrogate model and a genetic algorithm for improved computational time.

The diffuser augmented turbine was found to perform better in Yawed flows than a bare rotor turbine, with the performance being as close to the peak performance with a Yaw angle of $\pm$ 30^{o}.This performance is largely dependent upon the length to diameter ratio of

the diffuser. The wake recovery of diffuser augmented devices was found to be poor, with the wake velocity being less than half that of the bare rotor. More work must be done to improve the wake recovery of the Diffuser augmented turbine for possible array deployment.

Riglin J. et. al. [19] (2016) To determine the Performance predictions numerically for water current turbine arrays system for river applications. The simulations for the micro hydrokinetic arrays system are conducted with actual turbine geometries incorporated in the fluid domain, providing more accurate power and thrust results corresponding to a specific design rather than low accuracy models like Actuator Disk Model.

Reynolds Averaged Navier-Stokes equations were used to computationally characterize Multiple hydrokinetic turbines in three array configurations. The simulations were conducted for pre-existing turbines operating at their optimum power coefficient of 0.43 which was obtained by design and optimization process. Mechanical power for two adjacent units was predicted for various lateral separation distances. An additional two-by-two turbine array was studied, mimicking a hydro-farm.

Steady state simulations were conducted using both Coupled and SIMPLE pressure-velocity solvers. Steady three-dimensional flow structures were calculated using the k-u Shear Stress Transport (SST) turbulence model.

At a lateral separation distance of 0.5Dt, the turbines produced an average 86% of the peak power a single turbine producing. Interaction effects at lateral separation distances greater than 2.5Dt were negligible. The wake interaction behind the upstream turbines causes a significant performance reduction for downstream turbines within 6Dt longitudinal spacing.

Chica E. et. al. [20] (2016)To develop a rotor having an optimum geometry that can capture the maximum energy from the water. Horizontal Axis Hydraulic Turbine is selected over VAHT because of its inherent advantages that include: Easily self-starting, Less torque fluctuation, Higher efficiency, and operational ability at larger speeds.

A prototype turbine of 1 Hp (746 W) having 3 blades was designed for a water velocity of 1.5 m/s with a tip speed ratio λ= 6:325, an angle of attack of 5 and as the pitch angle Θ=

0□; and the Maximum Power Coefficientof the turbine was calculated, which was 0.4382, near the Betz limit. S822 airfoil was used to generate the coordinates of the blade. CFD simulation was carried out using Ansys CFX to estimate the performance of the blade design. Furthermore, FEM was successfully used for stress calculations on turbine blades under the influence of centrifugal and hydrodynamic loading. From the Cp (λ,Θ) versus λ characteristics for various values of Θ, it was observed that Cp has a maximum of 0.4382 when Θ= 0 and λ= 6:325.Thus for a given power output, the radius and the length of the blades can be obtained. In this work, a horizontal axis hydrokinetic turbine blade is designed and verified with the help of the momentum theory, the blade element momentum theory and numerical simulation. The optimum twist angle and chord length for each section of the blade were calculated using turbine output power, tip speed, aerofoil, water speed and efficiency, among others, as design parameters.

The finite element analysis indicates that the blade will satisfactorily support the force exerted on it under the combined effects of the centrifugal, gravitational and hydrodynamic loads studied.

Goltenbott U. et. al. [21] (2017) Tostudy the aerodynamic interactions by utilizing diffuser augmented wind turbines with a multiple rotor arrangement. In wind tunnel experiments, the aerodynamics of two and three DAWTs, spaced in close vicinity in the same plane normal to a uniform flow, have been analyzed. A C_i type diffuser with brim heights varying from 0.03 to 0.1 D_{throat} (3-10%) has been used in all of the rotors. Hot-wire techniques used to measure the flow speed near the gap between the DAWTs in a MRS. For gap ratios s/D between 0 and 0.5, conventional turbines and DAWTs showed an increase in power output. DAWTs show higher power increases than conventional turbines, reaching a maximum of 9% at a gap ratio, of s/D ¼ 0.15 between neighbouring brims. The power increase is further dependent on the brim height of the diffuser. The highest power increase was observed with a 10% brim height (CiB10).

Future work includes analyzing the in-field blockage and its effect on the power increase of each wind turbine in a MRS with side-by-side and vertically spaced wind turbines. Also,

CFD simulations could provide more details on the flow field, notably in regard to the gap between the turbines

Tampier G. et. al. [22] (2017): The objctive of the paper was to determine the interaction effects in a diffuser-augmented hydrokinetic turbine by utilizing the generalized actuator disc theory. The performance, thrust, and average flow speeds are obtained at the turbine plane in simulations performed in three comparable cases: bare turbine, bare diffuser and diffuser augmented turbine employing Transient RANS CFD methods. The computations were performed using CD-adapco'sSTAR-CCM software utilizing an implicit unsteady simulation. The design of the diffuser defined corresponds to a NACA 10510 profile of 2 meters of length that is rotated 15 °, in which the base of the turbine core is coincident with a vertical drawn in the middle of the same length. The turbine used is SANDIA MHKF1 hydrokinetic turbine.

It was found that because of the diffuser augmentation, the power extraction of the turbine was increased by 39.37%, while the thrust was increased by 26.15%. It was also observed that the interaction induction factor a_i has a significant effect on the system performance and that it remains nearly constant within the studied TSR range for the presented case.
The study of a series of different diffuser and turbine geometries could be done to develop a better understanding of the subject.

Maulana et. al. [23] (2018) In this study, flanges and a curved interior were added to an existing DWAT design. A CFD simulation is used to obtain the suitable shape or design of the micro-scale wind turbines. Geometry obtained by using a diffuser with curved interior diameter of 115 mm, length 230 mm, the tilt angle of 9° and flange height is 0.6 h / D. Using this geometry specification, wind velocity is increased up to 2.15 times than free stream velocity.

Chica E. et. al. [24] (2018) The manufacture and experimental evaluation of a hydrokinetic turbine of 1 kW are presented. A water velocity of 1.5 m/s, with a power coefficient of 0.4382, a tip speed ratio of 6.325, an angle of attack and pitch angle of 5 and 0 degrees, respectively, a blade length of 0.79 m, a drive train efficiency of 70% and a S822 hydrofoil profile were used for the design. The blades were designed and manufactured by Computer

Aided Design (CAD) and Computer Aided Manufacturing techniques (CAM) with a solid cross-section in order to provide the required strength. They were made of Prolon MS (Castnylon + Molybdenum). The platform that supports the turbine was a modular floating raft simple to install, flexible, and durable made of high density polyethylene resin. The supporting structure of the turbine generator was made of stainless steel. The turbine was constructed of high quality and durable materials. To determine the efficiency of the designed turbine, the electrical power and kinetic energy of the river were measured and overall equipment efficiency of 0.5359 was obtained

2.2 Motivation:

Indian states are full of canals used for irrigation and as water transport in different parts of the country. These waterways and canals play a very important role in irrigation of crops in several regions of India such as Rajasthan and Tamil Nadu.

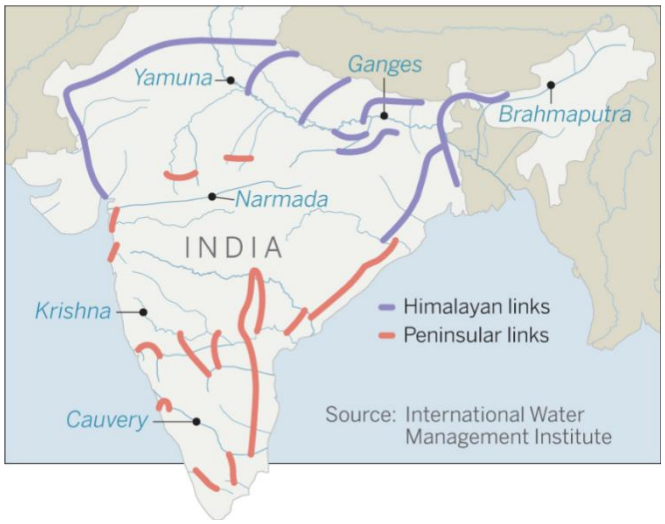

Fig. 2.3. Canals and Irrigation Channels in India (source: www.google.com)

Installing low-cost hydrokinetic turbines in these canals can prove highly beneficial and would reduce the operational load on conventional power generation units. Moreover, Duct Augmentation in these turbines can be done to further increase their efficiency. Also, Hydrokinetic energy is a Renewable form of energy, so it doesn't have any negative impact on the environment.

2.3 Research Gap: The efficiency of the hydrokinetic devices used can still be increased by employing new design techniques and using innovative techniques.

1. Most of the researchers have developed a computational model by varying one of the following parameters of the diffuser geometry: area ratio, diffuser angle, diffuser half-length, nozzle angle, nozzle half-length, interior profile, exterior profile of the diffuser or the addition of brims at outlet area.
2. Techniques like ADT (Actuator Disk Theory), BEM (Blade Element Modelling) and VBM (Virtual Blade Modelling) have been used to model the blades of the hydro-kinetic turbines.
3. The experimental analysis is generally performed in a wind-tunnel setup, or alternatively through the use of a hydrodynamic test canal where pressure and velocity measurements are done with the help of a Hot wire anemometer and a static pressure probe.
4. In most of the computational analysis, the diffuser is modeled as a simple cylindrical wall with a conical section. It is expected that a more streamlined design will perform better, such as a hydrofoil shape. [9]. More research is needed for the development of the diffusers with High lift aerofoil geometries which promise an increase in performance as compared to the conventional geometries. [6]
5. Some studies were conducted for enhancing the performance of a diffuser with an aerofoil shaped axi-symmetric flap (NACA 4412) and an increase in power output was observed, which was directly attributed to the change in the pressure field inside the shroud due to the presence of the aerofoil flap.[2]
6. It has been stressed by several researchers that further study is required in the development of such multi- hydrofoil diffusers as detailed investigation on optimal design, size and shape of such diffusers is still an unexplored domain.

In this project,the design and development of such a multi- slot aerofoil diffuseris attempted with the help of modelling and analysis software.

CHAPTER 3: THEORY OF DIFFUSER AUGMENTATION

3.1 Diffuser Augmentation based on momentum theory

Research was conducted by Oman and Foreman [3] in the field of wind turbine augmentation using a diffuser. When applied to a diffuser augmented hydrokinetic turbine, the one-dimensional momentum theory, following expressions are obtained. From Fig. 3.1, the ideal power coefficient C_{Pi}may be represented as:

$$C_{Pi} = \Delta P_{23} * V_2 / (\tfrac{1}{2} * \rho * V_0^3) \quad (1)$$

and

$$C_{Pi} = [1 - Ki - C_{P4}] - [1 - \eta_D * (1 - \lambda)^2] \varepsilon^3 \quad (2)$$

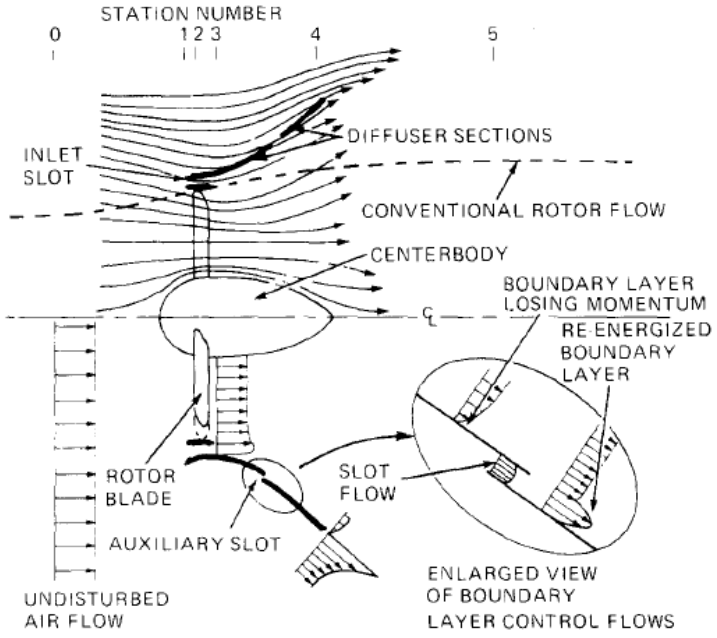

Fig.3.1. Diffuser augmented turbine showing reference positions

where ΔP_{23} – pressure drop occurring across the throat area, V_2 - the axial velocity at the blade tip, V_0 – the free stream velocity of the water, ρ – density of the fluid (water).

$\varepsilon = (V_2/ V_0)$, $\lambda = (A2/A4) = (A3/A4)$

Ki- (the total inlet pressure loss) / $(½ *\rho*V_0^3)$,

$C_{P4} = (P_4-P_0) / (½ *\rho*V_0^3)$,

$\eta D = (P_4-P_3) / ½* \rho*(V_3^2- V_4^2)$

It is clearly evident from equation (2) is that the power output that can be extracted by a ducted turbine may be increased significantly by using a diffuser with high efficiency ηD, a good velocity ratio and a strongly negative base pressure coefficient (C_{P4}), an optimum disk velocity ratio. For a given turbine placed inside the diffuser, the disk loading ($\Delta P_{23}/ (½ *\rho*V_0^2)$), is largely detrimental for obtaining the velocity ratio.

From the Betz Theory, the maximum power coefficient of a ducted(free) turbine can be obtained as 0.593, which represents the percentage of the maximum fluid kinetic energy that can be extracted by the turbine from the free-flowing stream.

The ratio of the power coefficient, r, of a ducted to the best unducted hydrokinetic turbine can be represented by the relative power coefficient given by:

$r = 1.6875 * C_{Pi}$ (3)

Based on the free stream velocities, and equal diameters of the turbine rotor, it can also be expressed as:

$$r = 1.6875 * C_T \left(\frac{1-C_{P_4}}{1-C_{P_R}+C_T}\right)^{\frac{3}{2}} \quad (4)$$

Where $C_T = \frac{p_2-p_3}{\frac{1}{2}\rho V_2^2}$

And $C_{P_R} = \frac{p_4-p_3}{\frac{1}{2}\rho V_3^2} = \eta_D \left[1 - \left(\frac{A_3}{A_4}\right)^2\right]$

Equation (4) has information about the inlet duct losses which are represented in the overall duct pressure recovery coefficient, C_{P4}. As the C_{P4} is practically unrelated to the

turbine load factor $C_{T,}$ the maximum augmentation ratio (maximum relative power coefficient) can be given by:

$$r_{max} = \frac{9}{8}\left(1 - C_{P_4}\right)\sqrt{\frac{1-C_{P_4}}{3\left(1-C_{P_R}\right)}} \quad (5)$$

the value of which coincides at the optimum load factor.

$$(C_T)_{opt} = 2 * (1 - C_{PR}) \quad (6)$$

Hence, it can be concluded from the given theory that greatest power augmentation of the hydrokinetic turbine can be achieved for

- The largest negative value possible for the diffuser exit plane pressure coefficient (i.e. diffuser exit pressure is reduced below atmospheric pressure)
- The largest diffuser pressure recovery coefficient possible.
- Induction of large volume flow through the rotor area, which can be observed from the relation between the diffuser pressure recovery and the turbine loading.

3.2 Reynolds Averaged Navier-Stokes Equation

Reynolds Averaged Navier-Stokes Equation equation is used for modelling of flow through all kind of fluid flow including open channel flow or flow through a river basin or flow of air through airplane wings. The generalized equation is complex in nature, and thus needs to be simplified for the purpose of its application to the problem of aerofoil.

Navier-Stokes equation in its generalized form can be written as:

$$\rho\left(\frac{Dv}{Dt}\right) = -\nabla p + \nabla \cdot T + f \quad (7)$$

where T is a symmetric tensor except for the condition when the fluid consists of a rotational degree of freedom.

The Reynolds-averaged Navier–Stokes equations (or RANS equations) are computed for average time for the motion of fluid flow. Reynolds decomposition allows an instantaneous quantity to be decomposed into its time-averaged and fluctuating quantities to describe turbulent flows.

These equations can be used in accordance with the application based on understanding of the characteristics of flow turbulence to estimate time-averaged solutions of the Navier–Stokes equations.

For an incompressible Newtonian fluid undergoing stationary flow, above mentioned equations can be expressed in Einstein notation as:

$$\rho \bar{u}_j \frac{\partial \bar{u}_i}{\partial x_j} = \rho \bar{f}_i + \frac{\partial}{\partial x_j} \left[-\bar{p}\delta_{ij} + \mu \left(\frac{\partial \bar{u}_i}{\partial x_j} + \frac{\partial \bar{u}_j}{\partial x_i} \right) - \rho \overline{u_i' u_j'} \right] \quad (8)$$

where the left-hand side of the equation denotes the change in average momentum of fluid element is equated to the mean body force, the isotropic stress due to the average pressure field, the viscous stresses and apparent stress due to the fluctuating velocity field, commonly referred to as the Reynolds stress.

CHAPTER 4: PROPOSED METHODOLOGY

4.1 Problem Statement

The performance of a simple diffuser can be augmented by using a secondary diffuser and with the help of profiles developed using a high-lift aerofoil geometry. The use of such high-lift aerofoils can prove to be largely helpful as they increase the mass of the water flowing through the turbine. This project focuses on the development of a Multi-slot diffuser model for the purpose of Velocity enhancement of axial hydrokinetic turbines operating in open channels.

4.2 Objectives

The main objective of the study is to obtain the following parameters from the analysis:

- Selection of a suitable high-lift geometry profile for the multi-slot diffuser model.
- Selection of an appropriate solver for the computational analysis.
- Selection of a suitable model to model the flowing water stream and tuning it for the analysis of the model.
- Establishing the convergence of solutions obtained using the analysis software.
- Comparison of the performance of the multi-slot diffuser models based on the results obtained by the Computational Fluid Dynamics analysis on ANSYS Fluent.
- Study of different parameters like: x-directional velocity, static pressure distributions to investigate the performance of the developed model.

4.3 Methodology

- Review of the different research conducted on the high-lift aerofoil geometry profile and selection of an optimum profile for the diffuser.
- Research on the different solvers used in the analysis e.g. Star CCM CD-adapco, Gambit, Ansys Fluent, ICEM CFD, Ansys CFX etc.
- Selection of an appropriate model for the flow modelling of the flowing stream.
- Establishing mesh convergence by using the iterative solver techniques.

4.4 Selection of the profile of diffuser

Research has already been done on the different aerofoil shroud geometries and their effect on the mass flow amplification through the turbine. The aerofoil geometries evaluated are E423, S1223, NACA0006, and F-74-CL5-140.

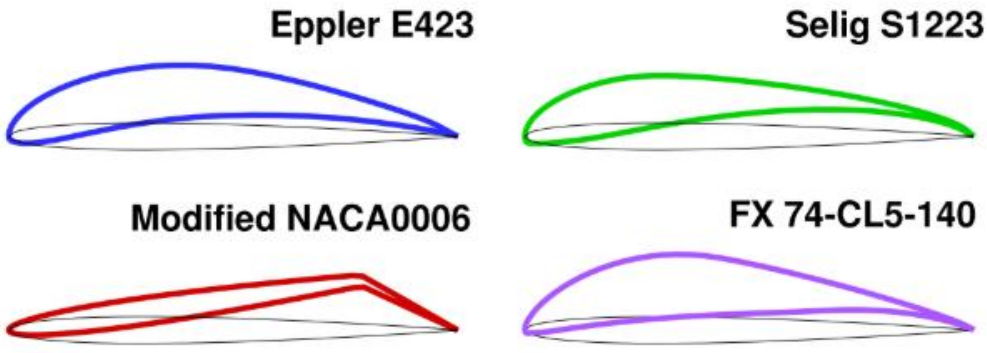

(a) Airfoil shapes

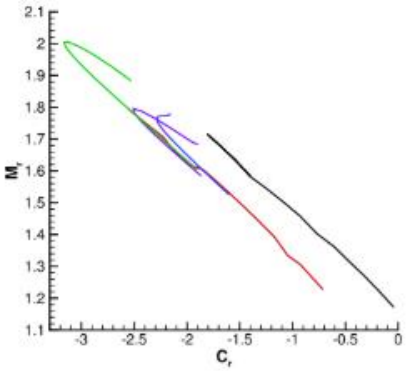

(b) Mass flow amplification M_r vs. radial force coefficient C_r

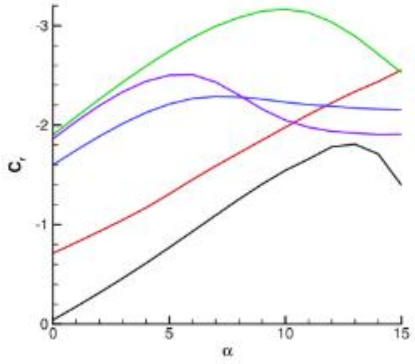

(c) Radial force coefficient C_r vs. angle of attack α

Fig.4.1 High lift aerofoil sections and their performances [16]

As evident from the Kutta-Jakouwski theorem, the mass flow amplification grows linearly with an increasing radial force coefficient. Of the airfoils considered, the Selig S1223 attained the largest mass flow amplification at an angle of 15^{o}, owing to the particular location of its stagnation point and hence this profile is selected for the development of base diffuser profile in our research work.

4.5 Development of CAD Model Geometry

In this research, the Aerofoil geometry selected for the multi- slot diffuser is Selig S1223, which is a High-lift, Low Reynolds number aerofoil. The major advantage of using this aerofoil is that it produces a very high lift at relatively low operational speeds of flow, which is ideal for river and canal applications.

The base diffuser profile having an Angle of attack equal to 15^{o} has been selected because of its tendency to induct maximum mass flow rate through the throat area increasing further the power output of the turbine.

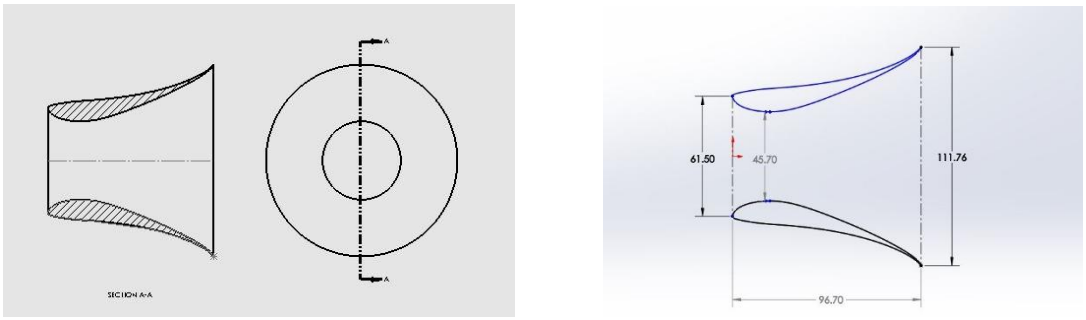

Fig.4.2 Base diffuser geometry (dimensions in mm)

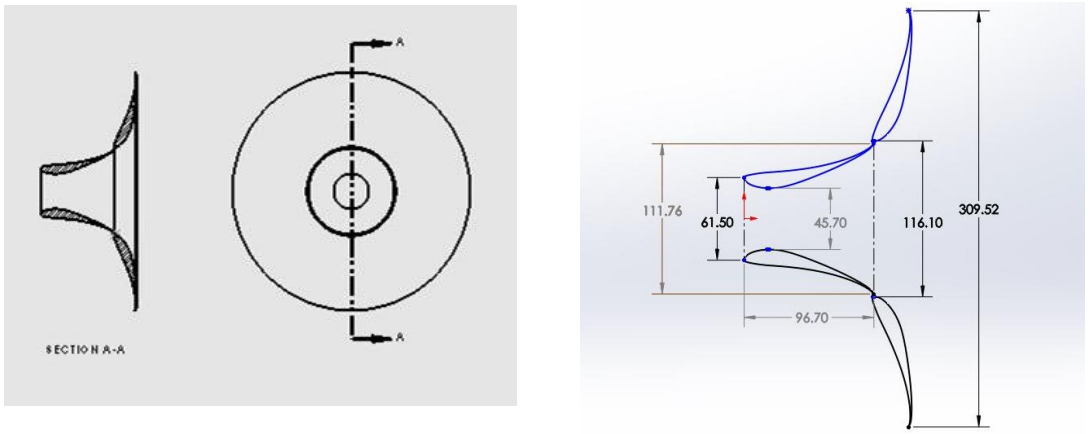

Fig. 4.3 Multi-slot diffuser geometry (dimensions in mm)

Same aerofoil section has been used for development of the second diffuser in this multi-diffuser turbine whose leading edge is located at an radial distance of 10% of the throat diameter from the trailing edge of the base diffuser.

The angle of attack of this secondary diffuser is varied from 0 deg to 90 deg (15^o, 30^o, 45^o, 60^o, 75^o) and the model is developed using Solidworks.

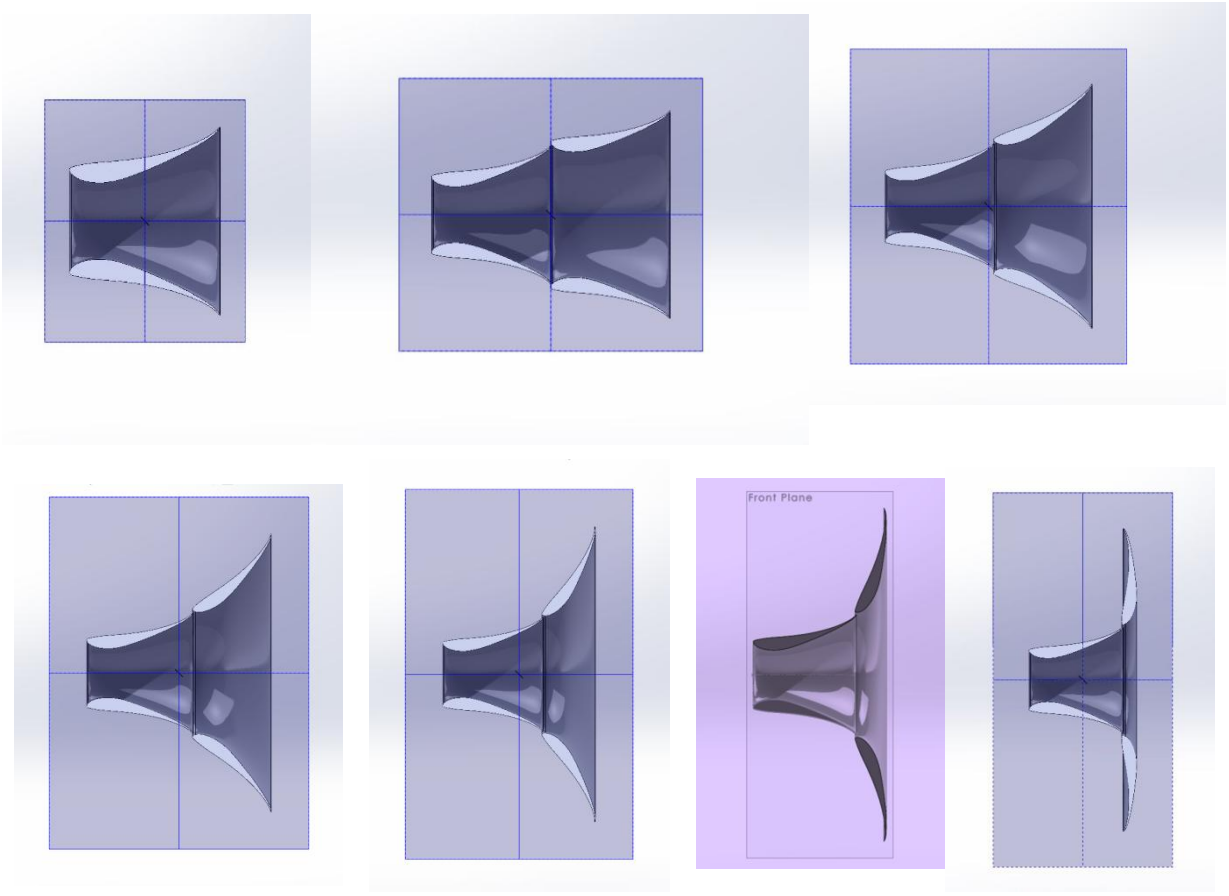

Fig.4.4. Different multi-slot diffuser geometries with increasing angle of attack of the secondary diffuser

CHAPTER 5

COMPUTATIONAL FLUID DYNAMICS ANALYSIS USING FLUENT

Ansys Fluent 18.1 is used to perform the finite volume analysis of the diffuser models. Following are the steps followed for the analysis:

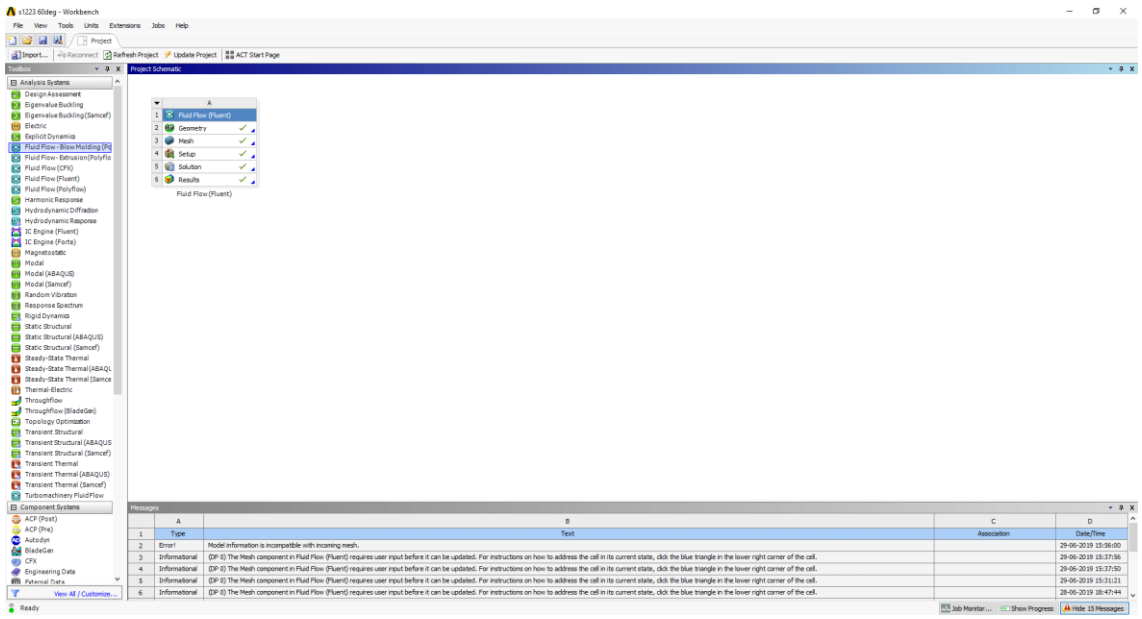

Fig.5.1. Ansys workbench with Fluent module

From the analysis systems drop down menu, select Ansys FLUENT as the solver for the analysis of the diffuser.

5.1 Pre-processing of the model: The pre- processing comprises of geometry definition, discretization of the model and selecting models and setting up boundary conditions for the model.

Geometry Definition: In the Geometry module, import the .IGES file of the diffuser model in the Design Modeler using Add geometry -> Import file. Some features might need to be edited after the geometry import e.g. split faces which can be done through the merge command. Further, the geometry must be frozen so that the solid part doesn't merge with the control volume surrounding the body.

An Enclosure which represents the fluid volume surrounding the diffuser model needs to be created around the diffuser in order for the solver to perform the analysis effectively.

The enclosure is a (2m* 1m* 1m) cuboid whose centroid coincides with the origin coordinate of the diffuser.

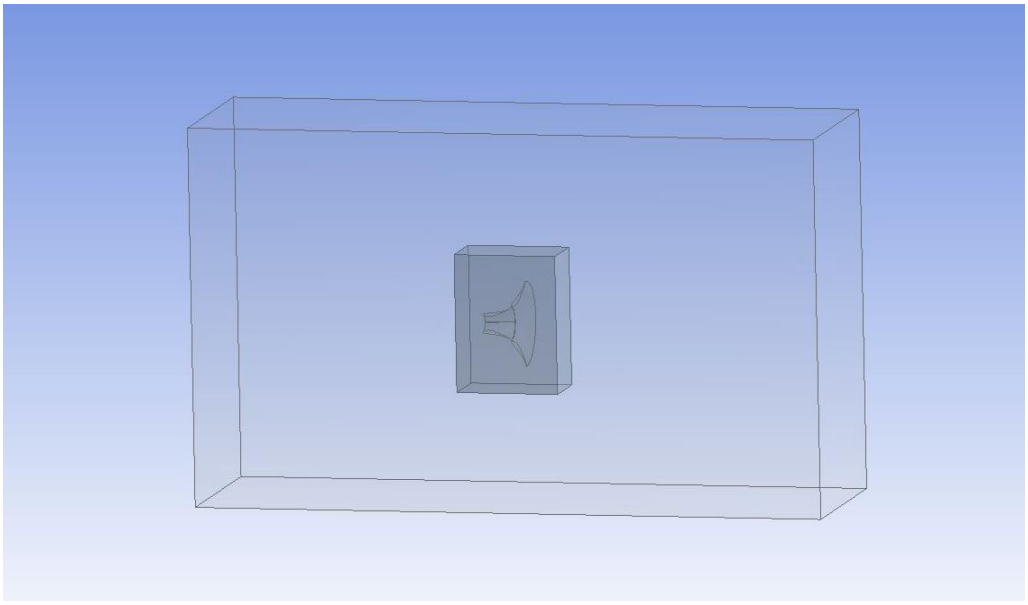

Fig. 5.2. Creation of an Enclosure around the diffuser geometry

Table 1. Details of enclosure

Shape	Box
Number of planes	1
Symmetry plane 1	ZX plane
Model type	Full model
cushion	Non-uniform
Cushion +X value (>0), FD1	1 m
Cushion +Y value (>0), FD2	0.5 m
Cushion +Z value (>0), FD3	0.5 m
Cushion -X value (>0), FD4	1 m
Cushion -Y value (>0), FD5	0.5 m
Cushion -Z value (>0), FD6	0.5 m

Further, a Boolean operation has to be performed which subtracts the Tool Body (diffuser) from the Target body (water).

5.2 Discretization of the Diffuser model: Meshing of the Diffuser model is done generally using CFD as Physics Preference and Fluent as the Solver preference.

The meshing of the fluid volume is done by using quadratic order elements due to the presence of complex curves in the geometry with the size function as Proximity and Curvature, medium relevance centre with a Growth rate of 1.188. The transition is kept as Slow with the 5 minimum cells across the gap.

Table 2. Details of mesh

Size function	Proximity and curvature
Relevancecenter	medium
Transition	slow
Span angle center	Fine
Curvature normal angle	Default (14.160^{o})
Num cells across gap	Default (3)
Proximity size function sources	Faces and edges
Min size	Default (8.8325e-005m)
Proximity min size	Default (8.8325e-005m)
Max face size	Default (8.8325e-003m)
Max tet size	Default (1.7665e-002m)
Growth rate	Default (1.1720)
Automatic mesh based defeaturing	on
Defeature size	Default (4.4162e-005m)

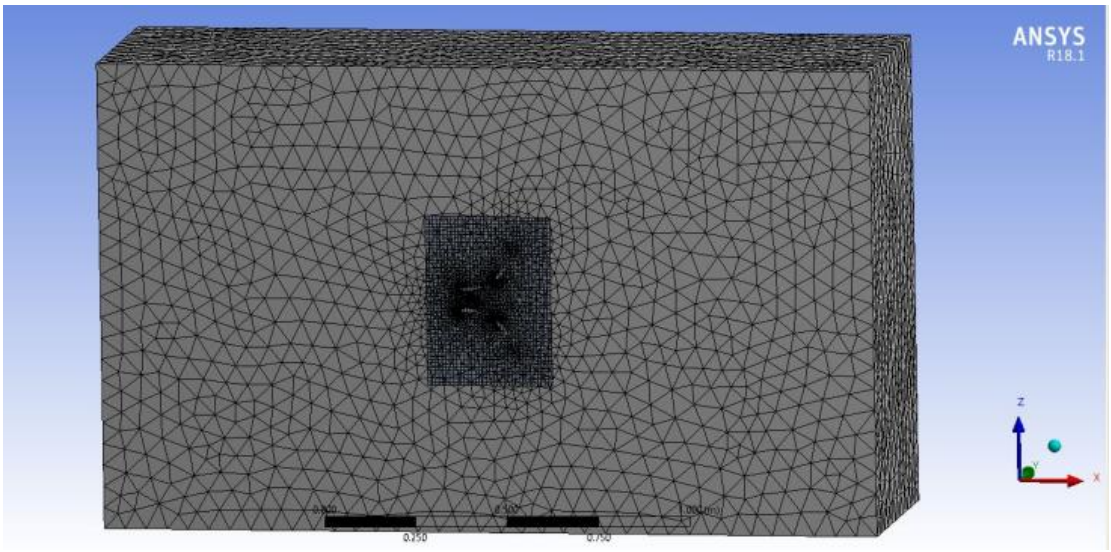

Fig.5.3. Discretization of diffuser model

Body sizing around the diffuser element is done to enhance the mesh size around our region of interest i.e. the area in close proximity around the diffuser. The element size in this area is kept lower than the size of the global mesh (element size= 1e-002 m) with a growth rate of 1.188.

Named Selections are created in order to allot different names to different regions of the geometry e.g. Velocity Inlet, Pressure outlet, walls and the diffuser geometry etc.

5.3 Setup of Computational Model

General setup: The fluid is modelled as incompressible through the help of pressure-based model, which is Transient in nature. The effects of gravity have also been considered.

5.3.1. K-ε Turbulence Model:

K-epsilon viscous model or K-ε turbulence model is the most effective model for the analysis of mean flow characteristics for turbulent flows condition and for this reason, most computational domain analysis is done using this model. K-ε turbulence model generally provides an estimation of turbulence with the help of two transport equations (partial differential equations).Generally, tis model is well suited for free stream conditions.

The K-epsilon model offers certain advantages over other turbulent models like mixing-length models, It can be used very efficiently well as to find a substitute to algebraically prescribed turbulent length scales in moderate to high complexity flows.

- Turbulence kinetic energy (k) is the primary transported variable.
- Rate of dissipation of turbulence energy (ε) is the secondary transported variable.

Table 3: Details of the viscous model

MODEL	K-epsilon viscous model
Type of model	Realizable model
Near- wall treatment	Scalable wall functions
Cmu	0.09
C1-Epsilon	1.44
C2-Epslion	1.92
TKE Prandtl Number	1
TDR Prandtl Number	1.3

Cell zone conditions: There are two fluid regions: one is the overall enclosure and the other one is the region of vicinity surrounding the diffuser. Both of these regions are said to be comprised of water (in liquid state at standard temperature and pressure)

5.3.2. Boundary conditions

Velocity Inlet- The region before the diffuser is selected as velocity inlet with the fluid flow towards the positive X-direction the flow velocity being V_0 = 5 m/s with Turbulent Intensity = 5 % and Turbulent Viscosity Ratio being 10.

Pressure Outlet: The gauge pressure is fixed as 0 Pascal. It has to be noted that ANSYS does all the calculations on the gauge pressure

The total pressure can be obtained by adding the Gauge pressure obtained with operating pressure (101325 Pascal).

The side surface as well as the bottom surface is modelled as a wall with specified shear of 0 Pascal.

Table 4: Boundary conditions at different zones

ZONE	Boundary conditions
Inlet	Velocity = 5 m/s
Outlet	Pressure = 0 Pa
Walls	Stationary wall, Specified shear (0,0 Pa)
Aerofoil diffuser	Stationary wall, No slip condition

Solution Methods:

Table 5: Solver settings

Type of solver	Pressure-velocity coupled solver
Spatial Discretization	
Pressure	Second order
Momentum	Second order upwind
Turbulent Kinetic Energy	First order upwind
Turbulent Dissipation Rate	First order upwind

5.3.3. Hybrid Initialization:

ANSYS Fluent offers another alternative to hybrid initialization models including standard initialization and FMG initialization. It is an amalgamation of recipes and boundary interpolation methods which solves Laplace's equation to estimate the velocity and pressure fields. All other variables including temperature, turbulence, species fractions, volume fractions etc. will be automatically compiled depending upon averaged domain values.

5.3.4 Calculations

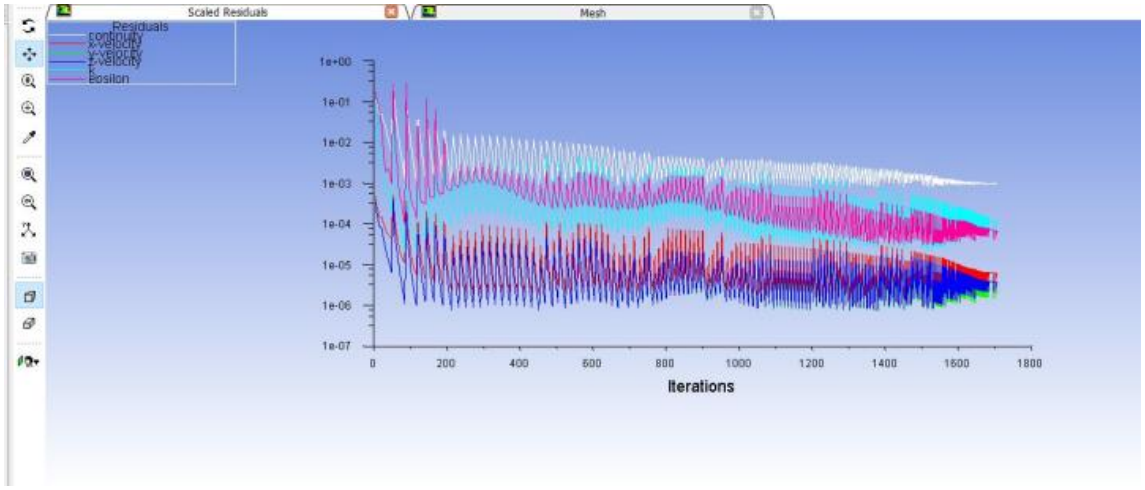

Fig.5.4. Calculation of the model with the given solver

The final calculation after initialization is performed with the following parameters:

Table 6 – Initialization details

Time step size (s)	0.005 seconds
Number of time steps	200
Maximum iterations/ time step	50

The residuals graphs show convergence with the increase in the number of iterations. In iterative solver methodology, initial guess is made (say u_0) and then solution is progressed and next better value u_1 is found then u_2 and so on till

$Ku_n - F = 0$ Where n = 0, 1, 2, 3, ……

Hence, this solving technique gives us an approximate result.

CHAPTER 6: RESULTS AND DISCUSSIONS

6.1 Post-processing of the ANSYS Fluent results

The results obtained from the Computational fluid dynamics analysis of the base diffuser and the different multi-slot diffuser geometries with increasing angles of the secondary diffuser profile are shown below:

CASE 1: Base diffuser

The base diffuser geometry is generated using the Selig S1223 profile as optimized by Aniket et. Al. [16] and the analysis is done using k-Ɛ turbulence model using a pressure-based solver.

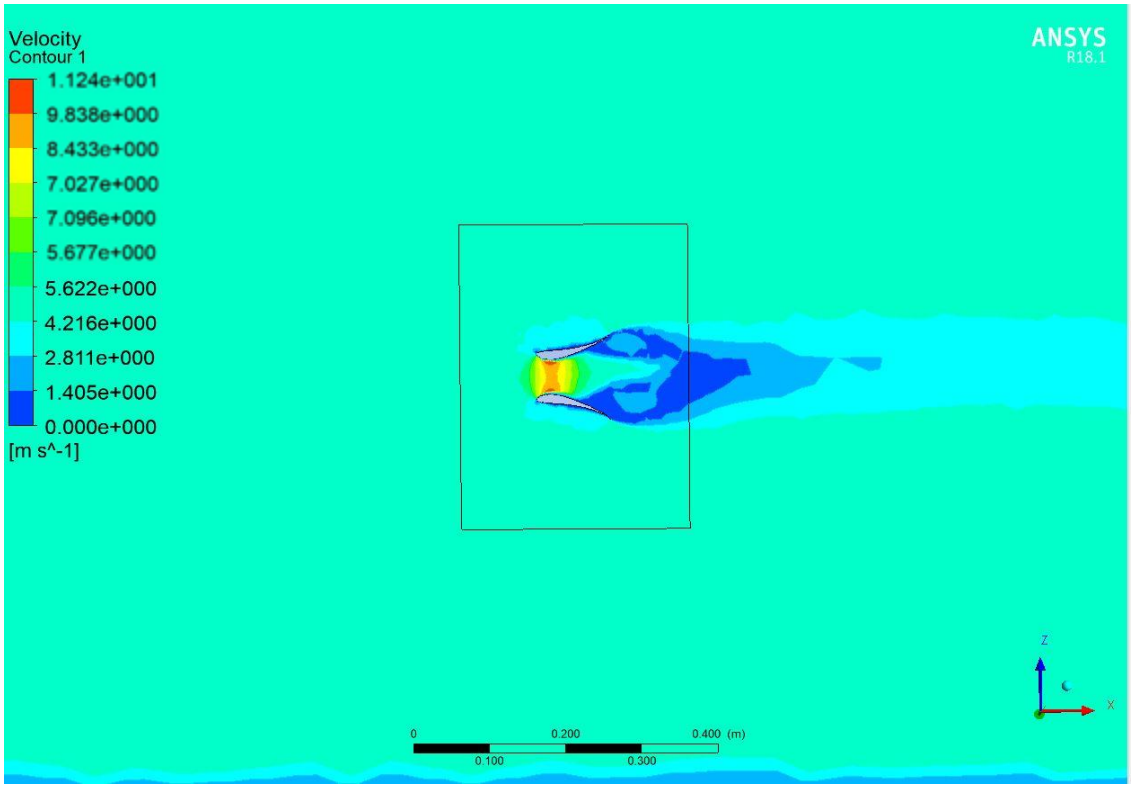

Fig.6.1. X-directional velocity component variation along the direction of flow

The maximum velocity is obtained in the throat region and the magnitude of this velocity is equal to 11.05 m/s.

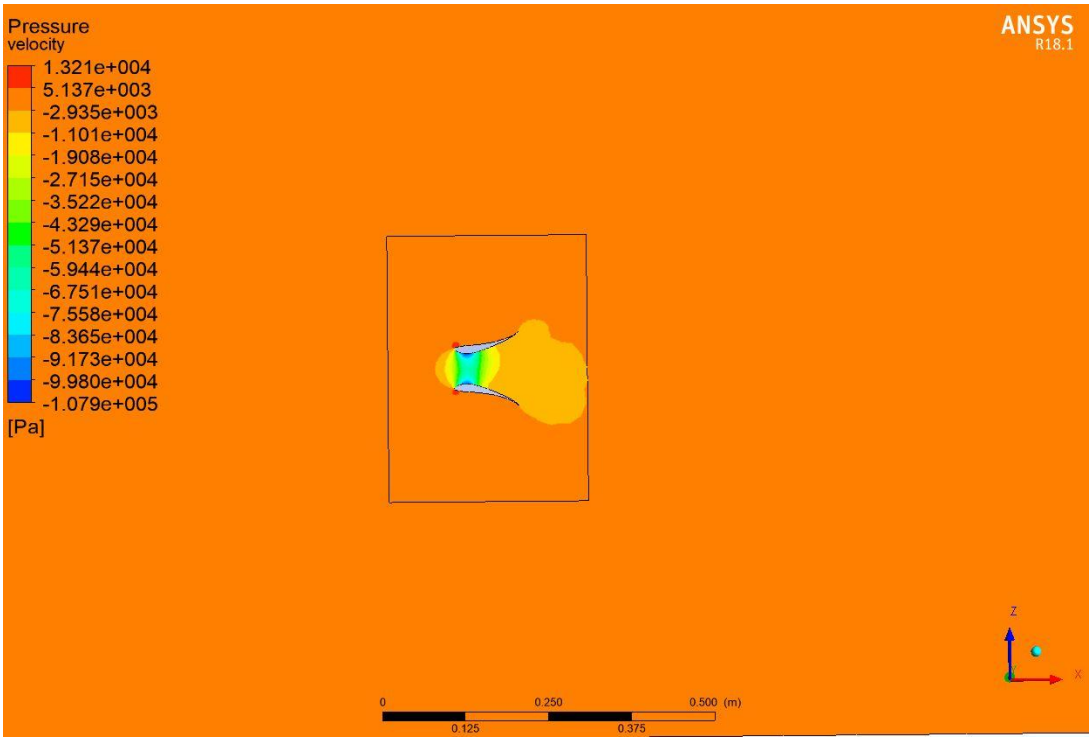

Fig.6.2. Static pressure distribution variation along the direction of flow

CASE 2: Multi- slot diffuser with secondary diffuser angle 15 deg.

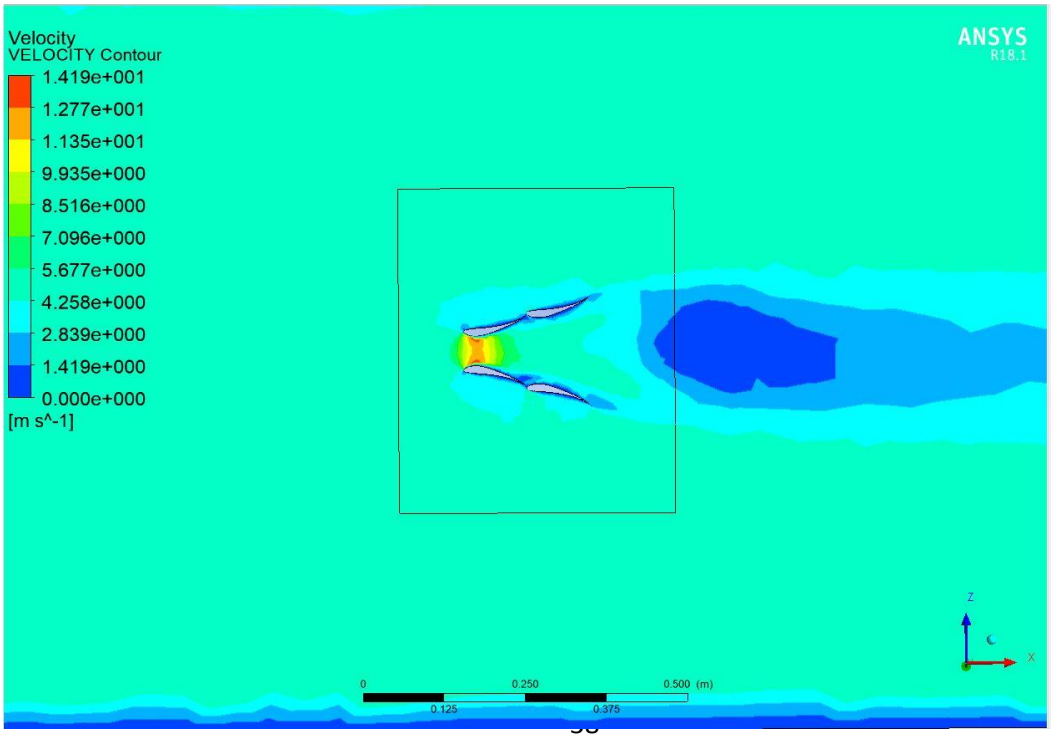

Fig.6.3. x-directional velocity component variation along the direction of flow

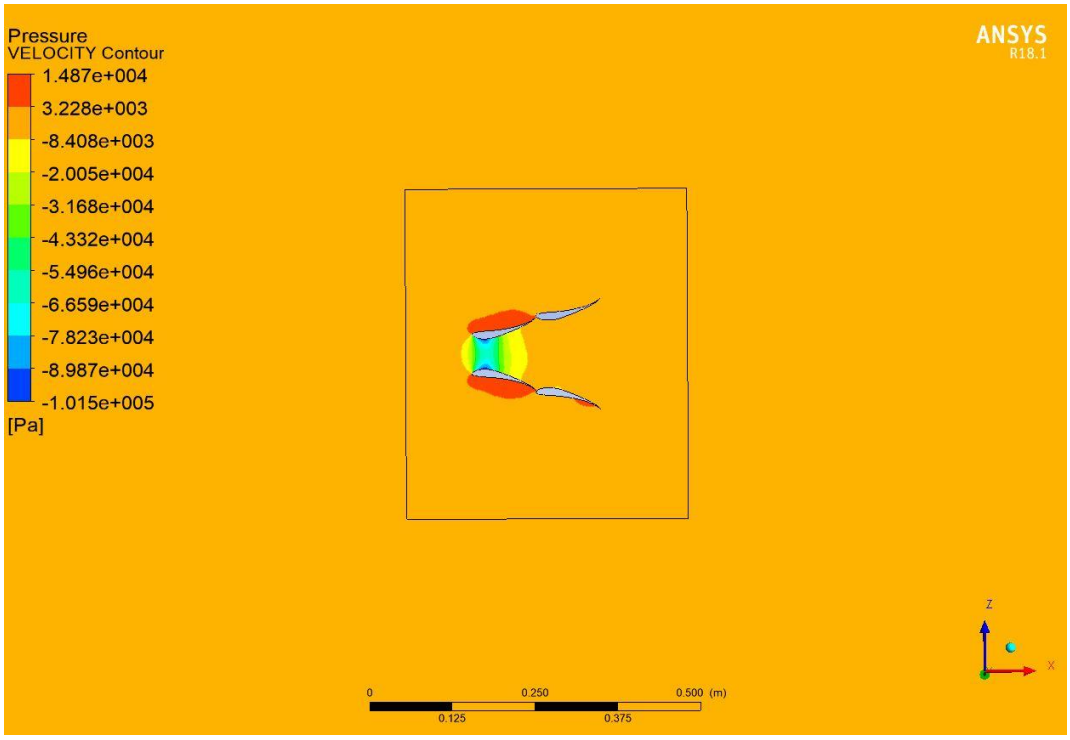

Fig.6.4. Static pressure distribution variation along the direction of flow

CASE 3: Multi- slot diffuser with secondary diffuser angle 30 deg.

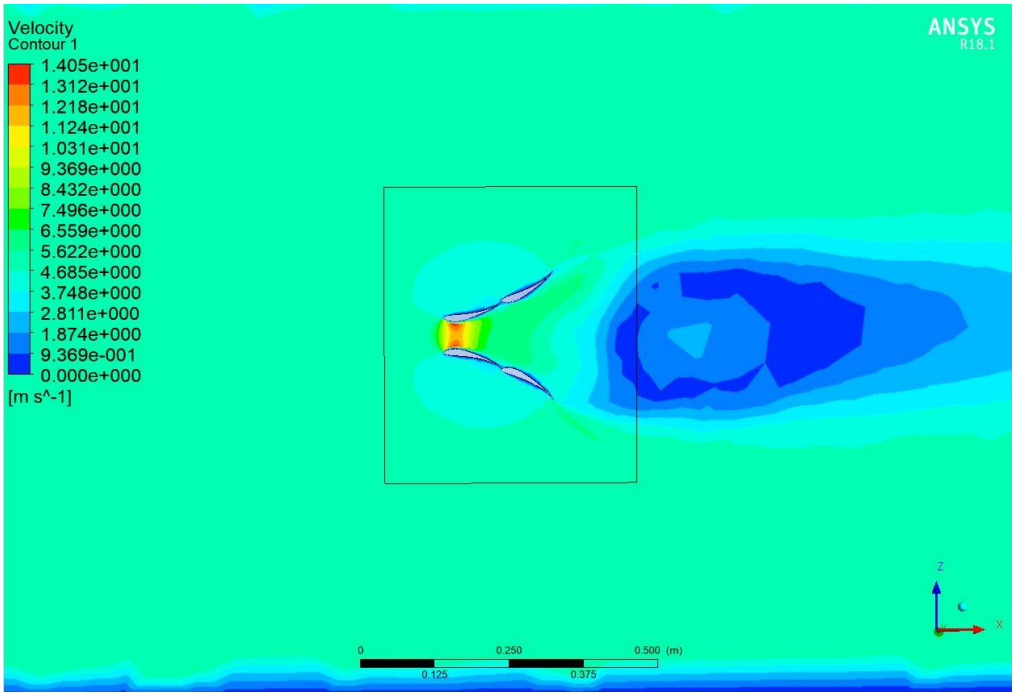

Fig.6.5. X-directional velocity component variation along the direction of flow

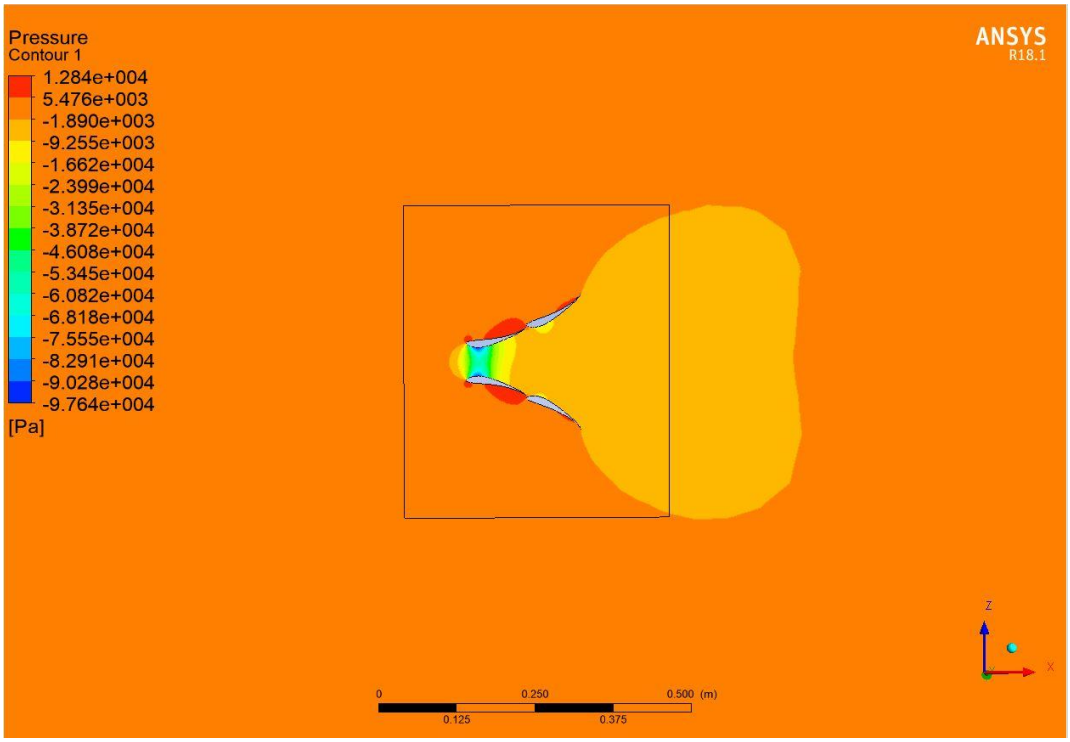

Fig.6.6. Static pressure distribution variation along the direction of flow

CASE 4: Multi- slot diffuser with secondary diffuser angle 45 deg.

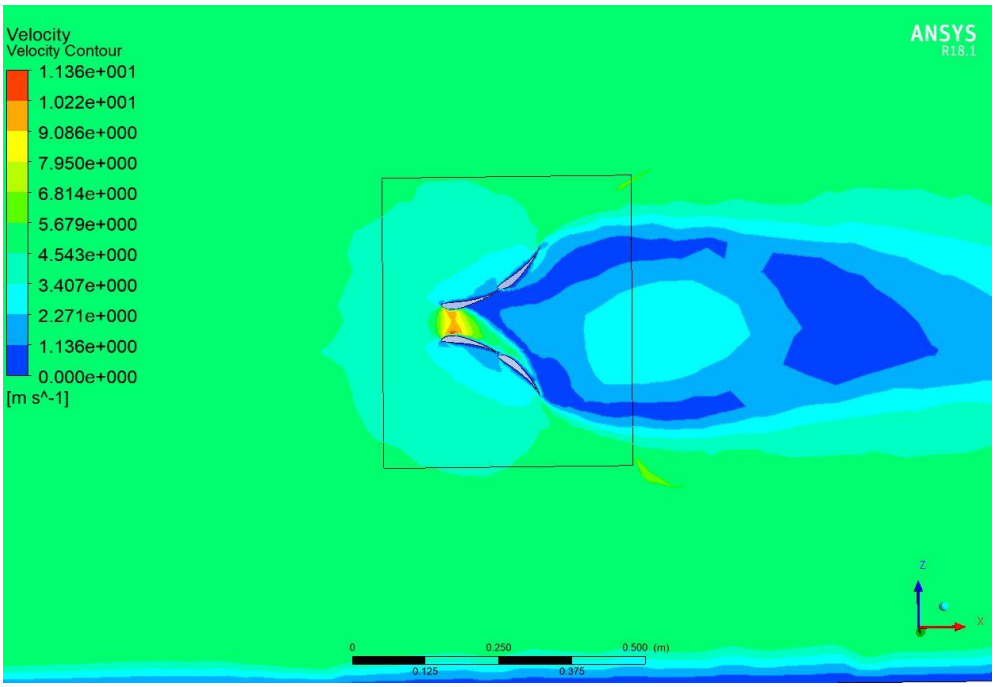

Fig.6.7. X-directional velocity component variation along the direction of flow

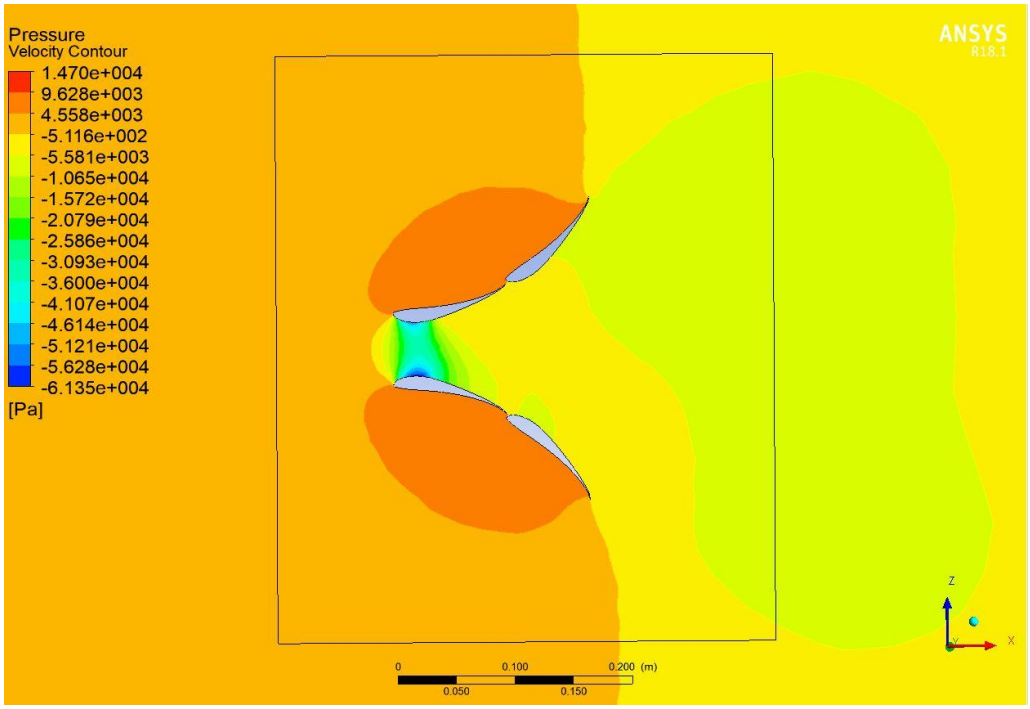

Fig.6.8. Static pressure distribution variation along the direction of flow

CASE 5: Multi- slot diffuser with secondary diffuser angle 60 deg.

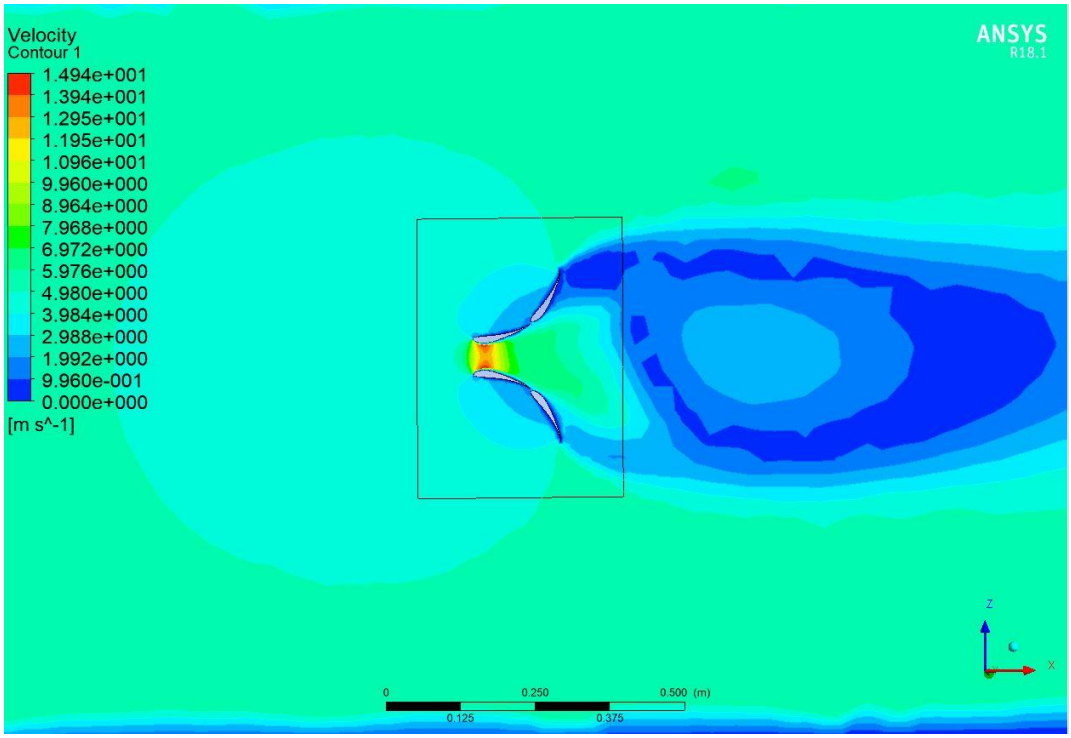

Fig.6.9. X-directional velocity component variation along the direction of flow

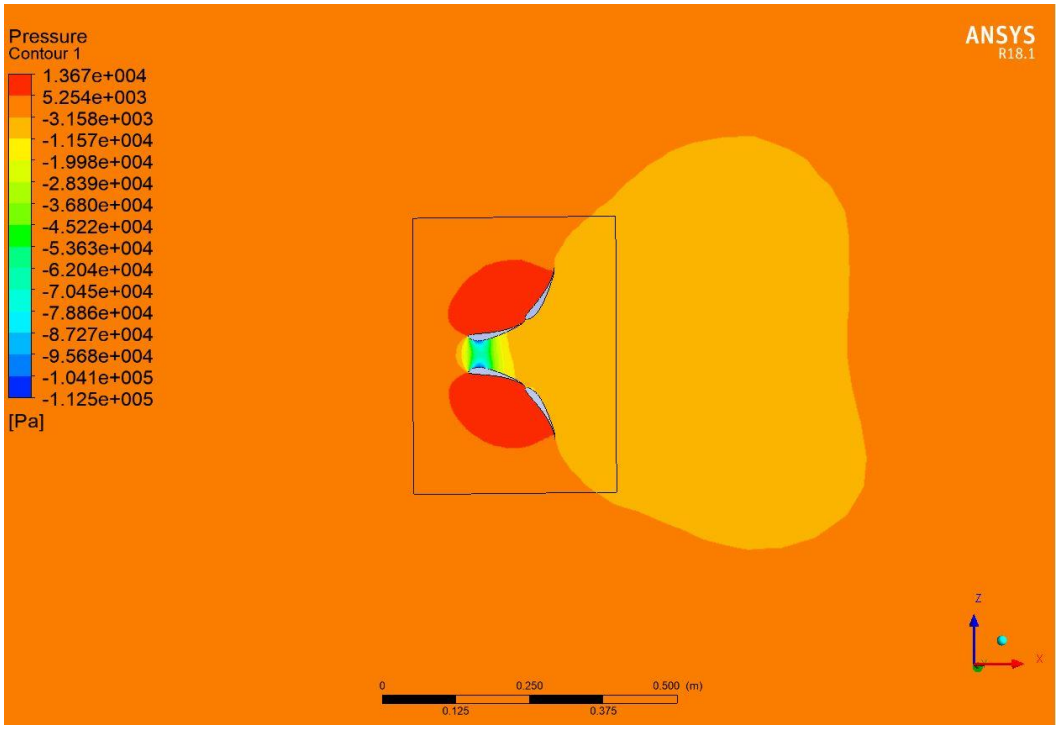

Fig.6.10. Static pressure distribution variation along the direction of flow

CASE 6: Multi- slot diffuser with secondary diffuser angle 72.5 deg.

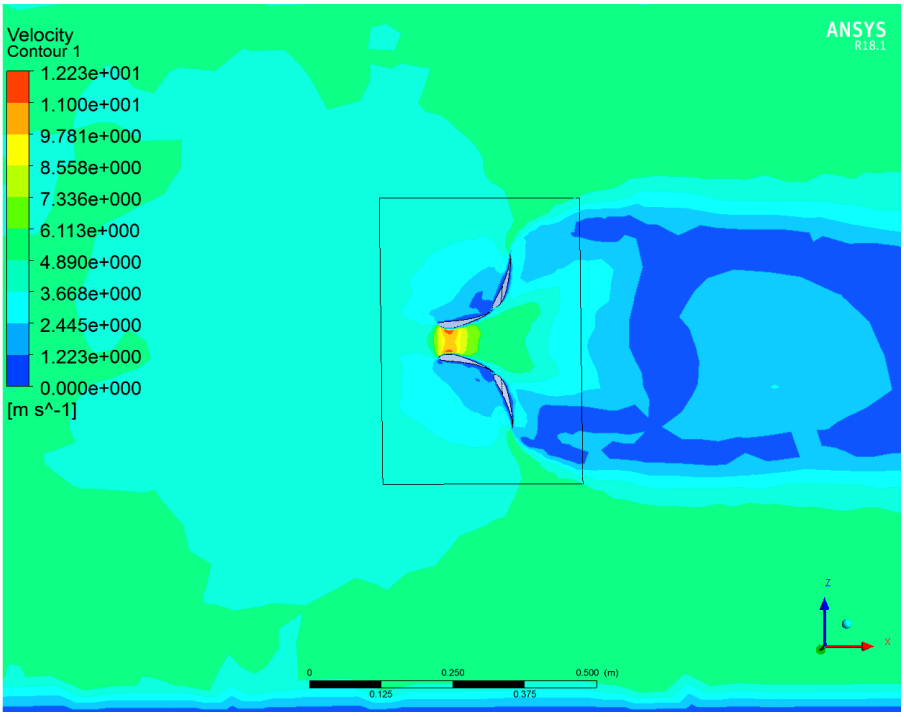

Fig.6.11. X-directional velocity component variation along the direction of flow

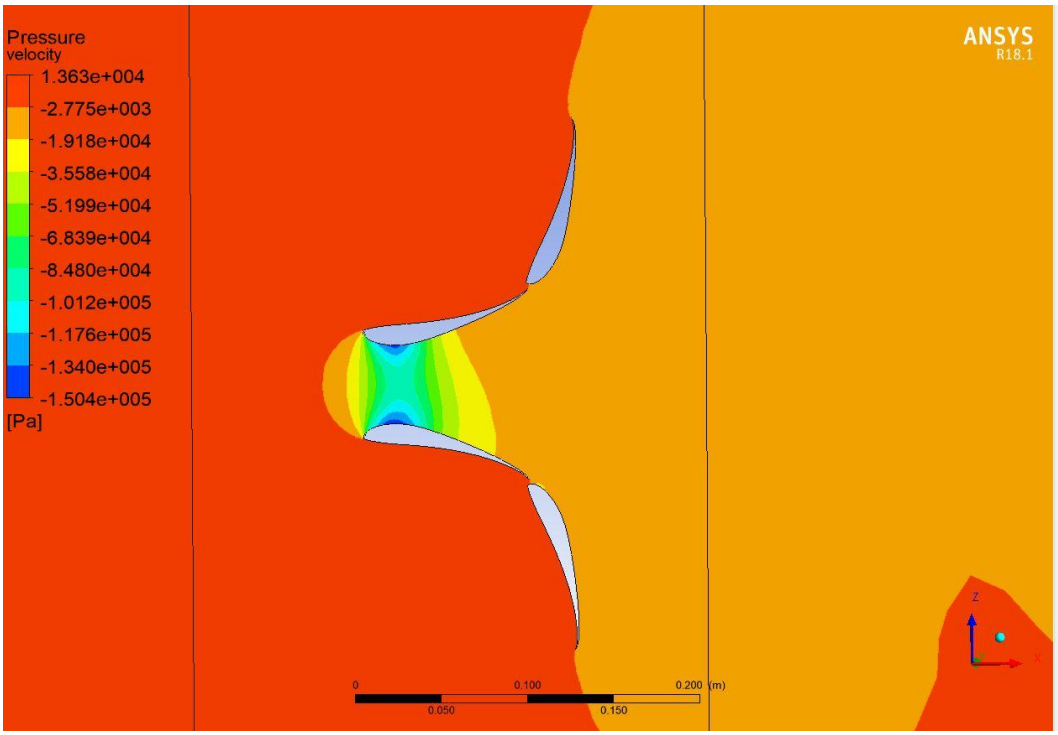

Fig.6.12. Static pressure distribution variation along the direction of flow

CASE 7: Multi- slot diffuser with secondary diffuser angle 75 deg.

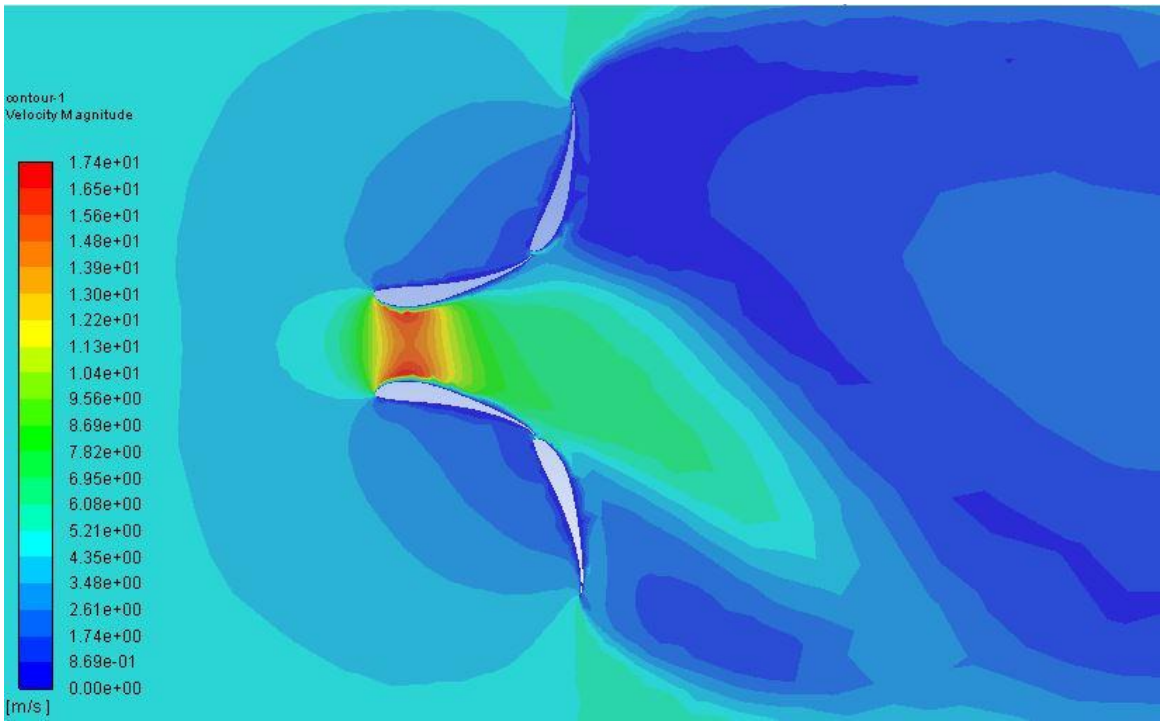

Fig.6.13. X-directional velocity component variation along the direction of flow

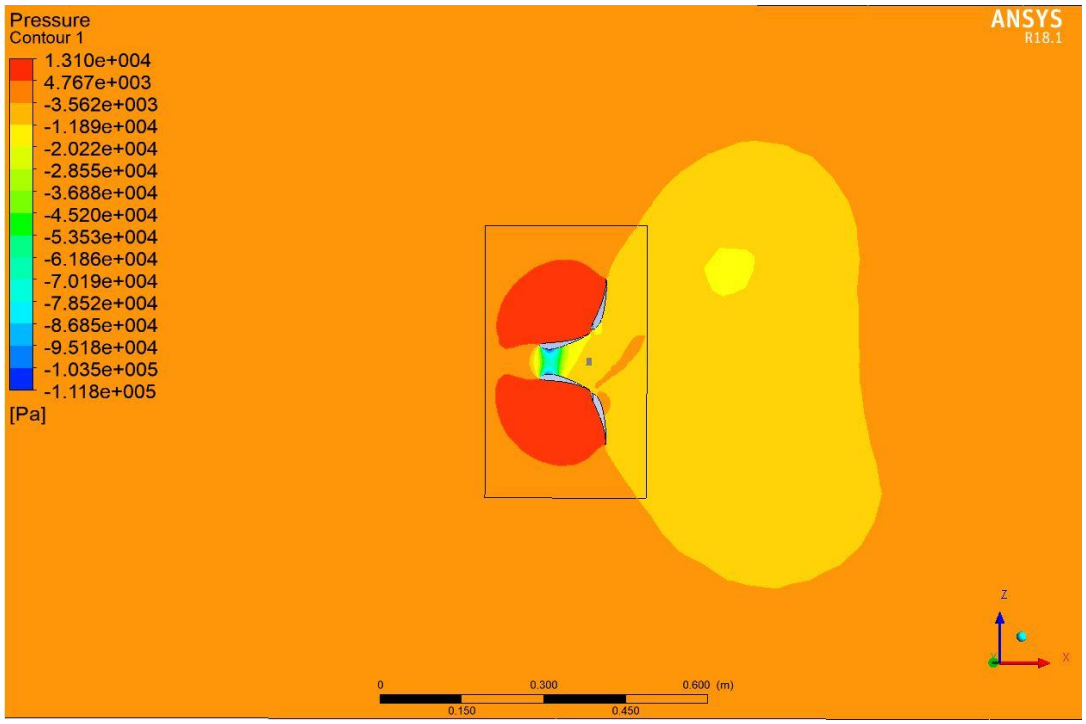

Fig.6.14. Static pressure distribution variation along the direction of flow

CASE 8: Multi- slot diffuser with secondary diffuser angle 77.5 deg.

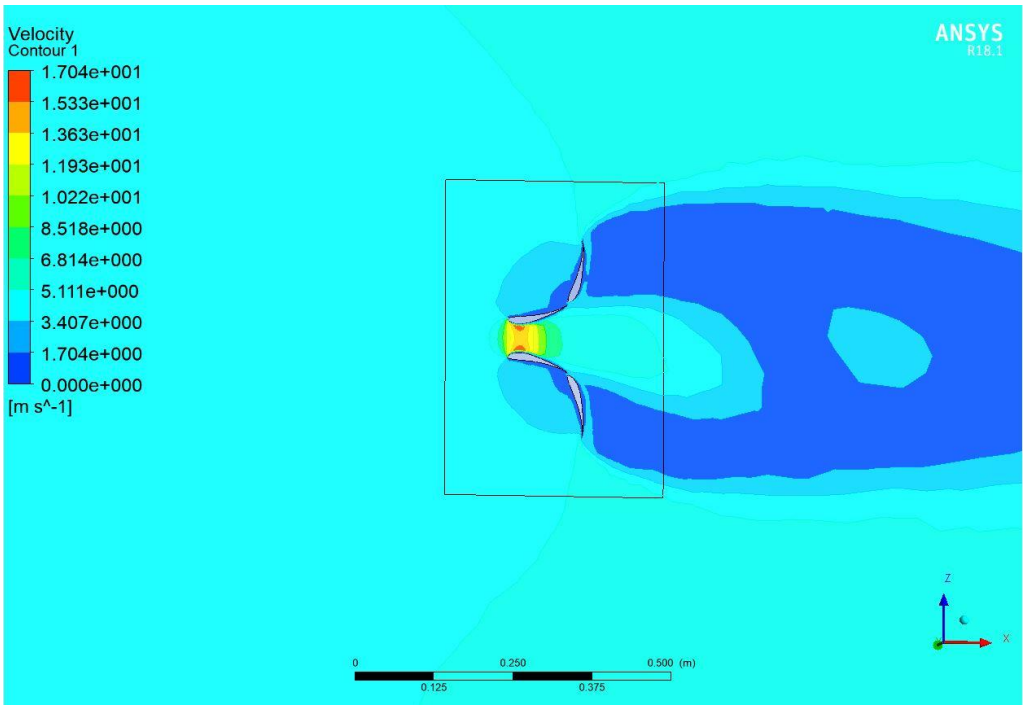

Fig.6.15. X-directional velocity component variation along the direction of flow

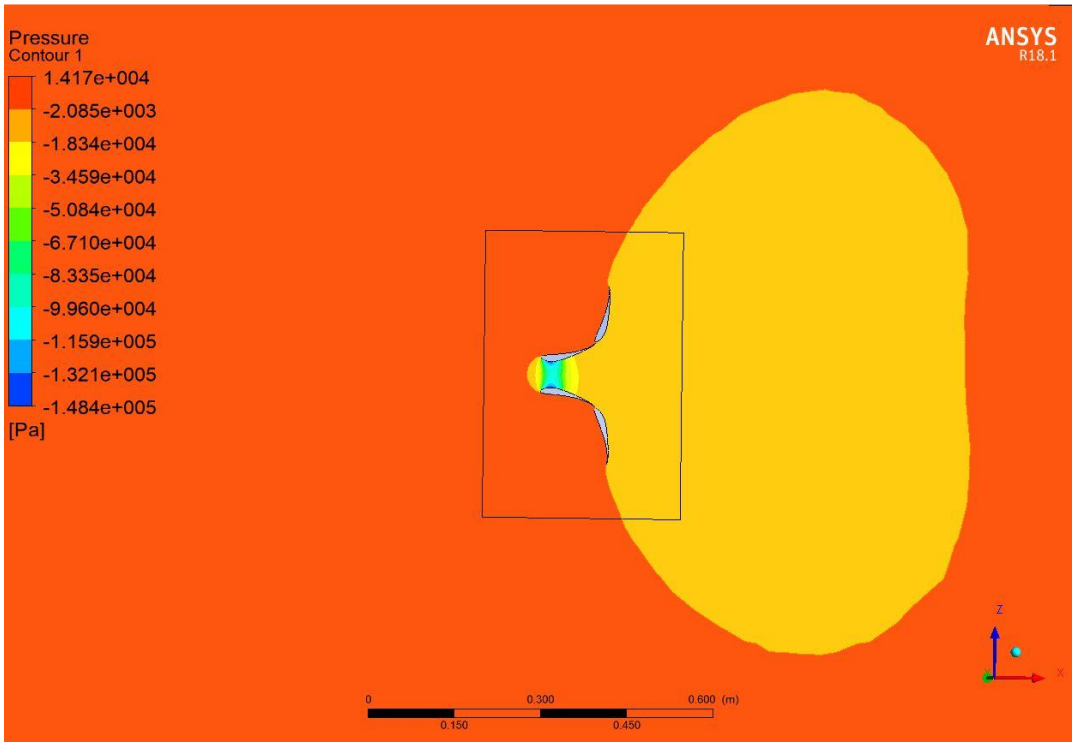

Fig.6.16. Static pressure distribution variation along the direction of flow

CASE 9: Multi- slot diffuser with secondary diffuser angle 90 deg.

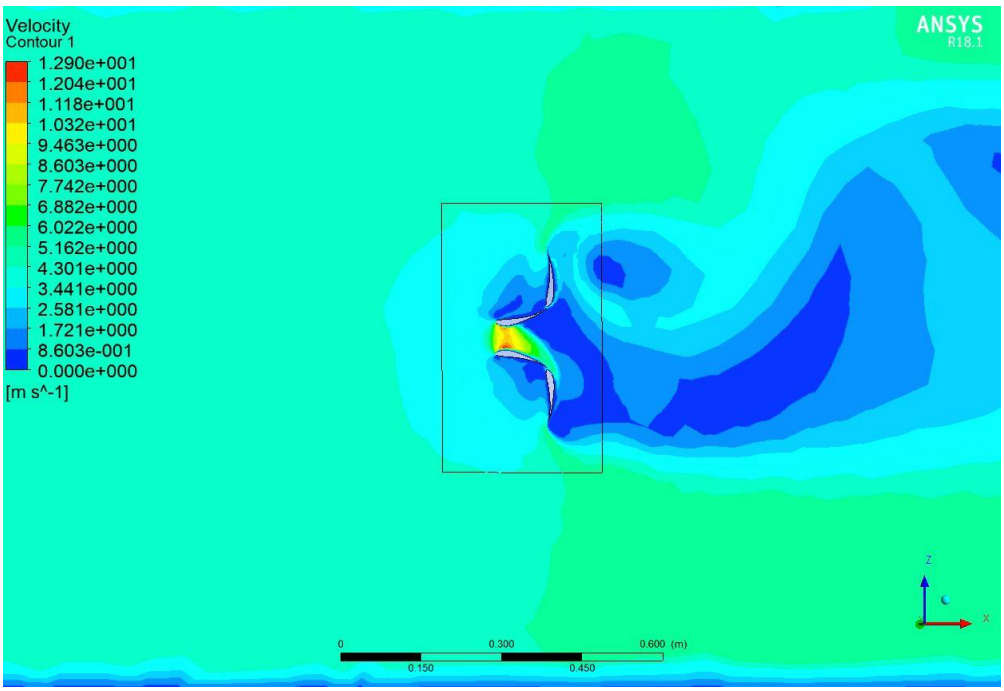

Fig.6.17. X-directional velocity component variation along the direction of flow

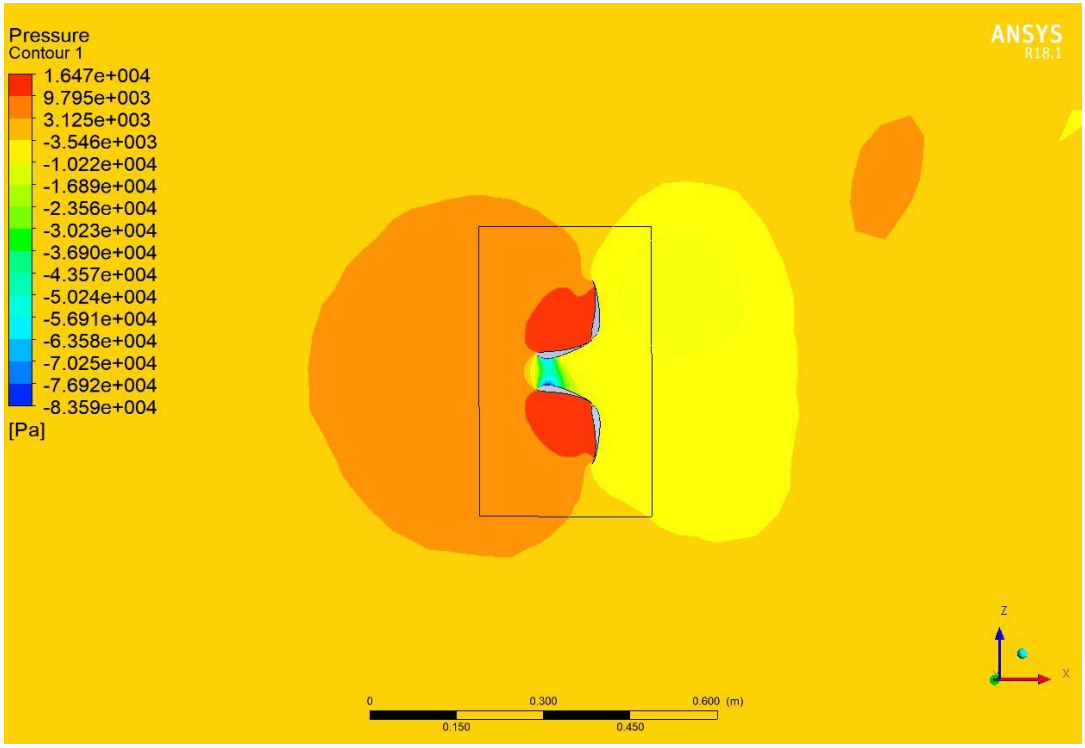

Fig.6.18. Static pressure distribution variation along the direction of flow

6.2 Analysis of X-directional velocity component along the throat area.

Analysis of the x-directional velocity component is done along the throat area sections of all the different diffuser profiles.

Table 7: Variation of the Velocity at throat with varying angles of the secondary diffuser

CASE No.	Angle of attack of secondary diffuser	Velocity magnitude (V_t) in m/s	Magnification factor = (V_t/V_0)
1	-	11.20	2.04
2	15	14.19	2.838
3	30	14.05	2.81
4	45	11.36	2.272
5	60	14.94	2.988
6	72.5	12.23	2.446
7	75	17.45	3.49
8	77.5	17.04	3.408
9	90	12.09	2.418

- The base diffuser has a maximum velocity at throat area equal to 11.2 m/s as concluded from the computational analysis.
- This gives a velocity magnification factor of 2.04 for the base diffuser.
- Of all the different profiles used for the multi- slot diffuser, the one with the angle of the secondary diffuser equal to 75 deg is found to have the maximum velocity at the throat. The magnitude of this velocity is 17.45 m/s
- This gives a velocity magnification factor of 3.49 for the 75 deg diffuser, which is a significant improvement over the base diffuser profile.

- This improved Velocity magnification factor can give better values of Power and Thrust coefficients, if the experiment is repeated with a turbine rotor installed at the throat area of the turbine.

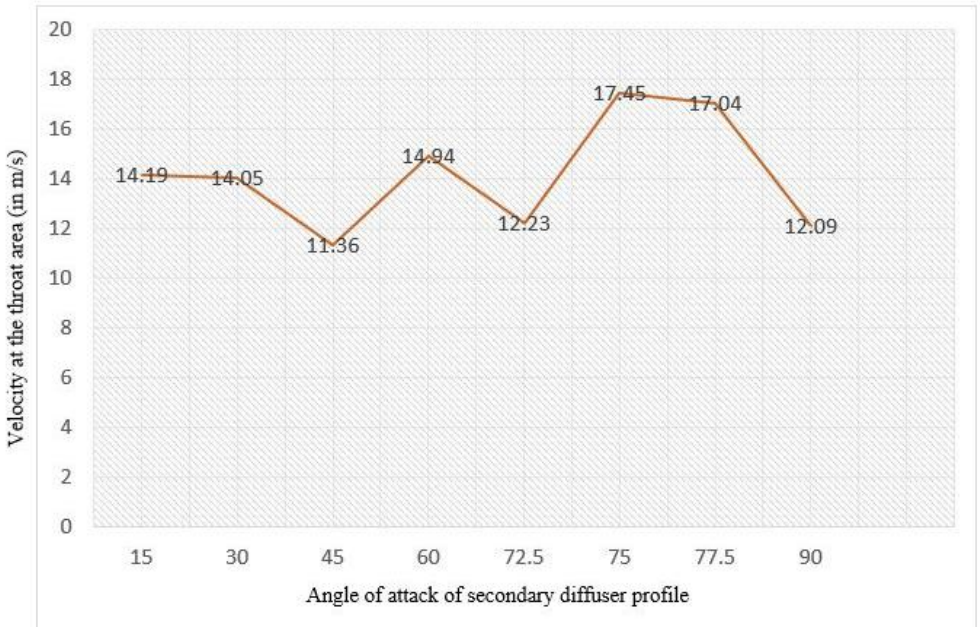

Fig 6.19 Graph showing the variation between the x-directional velocity with the increasing Angle of attack of the secondary diffuser profiles.

6.3 Mesh Convergence:

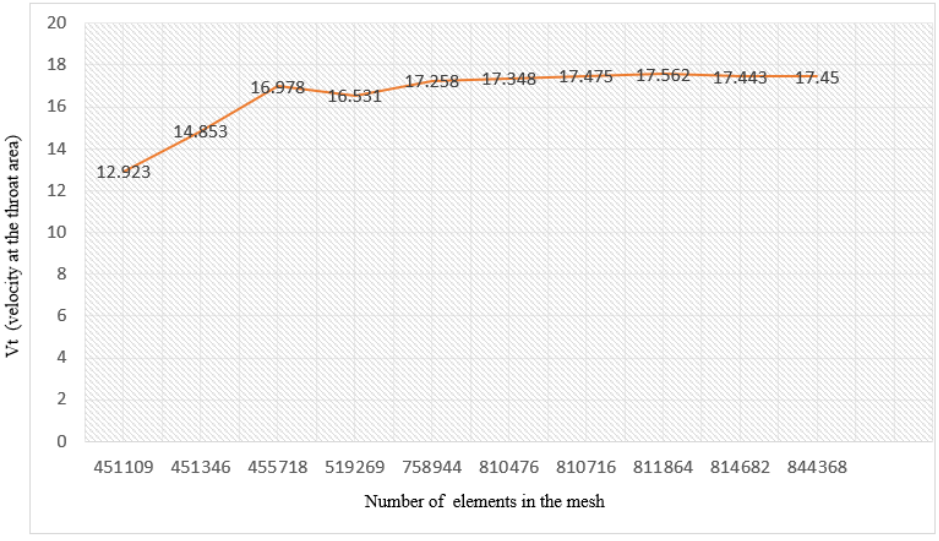

Fig. 6.20. Graph showing the variation between the x-directional velocity with an increasing number of elements

Mesh convergence is achieved by varying the number of elements of the mesh by varying different parameters of the mesh namely; Mesh details, Sizing method, grain size etc. Results were found to be independent of the mesh size as number of elements increased as shown in Table 8.

Table 8: Mesh Convergence

Number of nodes	V_t
451109	12.923
451346	14.853
455718	16.978
519269	16.531
758944	17.258
810476	17.348
810716	17.475
811864	17.562
814682	17.443
844368	17.45

6.4. Analysis of Static Pressure distributions along the inlet and at the exit of the diffuser

Case 1: Analysis of static pressure at the exit of the base diffuser (x=0.097m,y= 0m, z= 0 m)

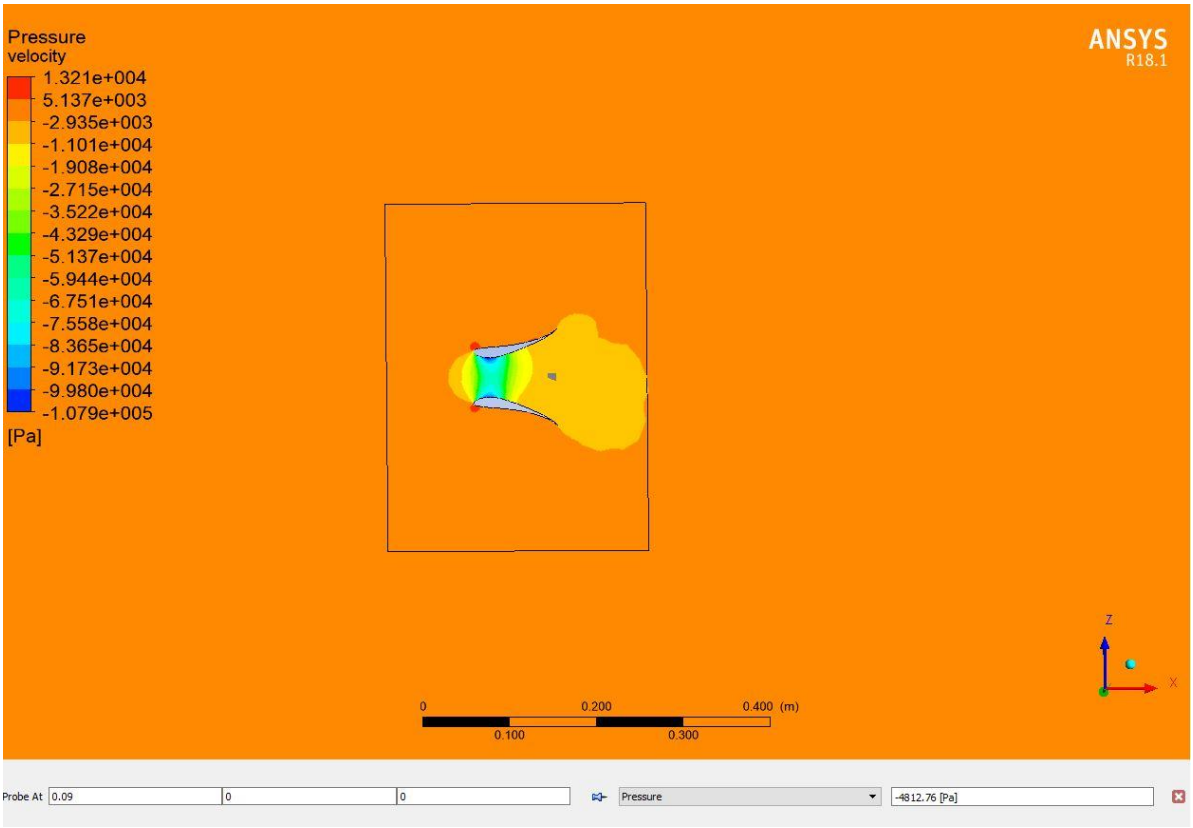

Fig 6.21 Probe at x=0.097m showing the pressure at the diffuser exit area

The static pressure at the diffuser exit is determined by using the probes at a distance of (x=0.097m,y= 0m, z= 0 m) and the value of P_{exit} is found to be equal to -4812.76 Pa.

- The inlet pressure at the entry P_0 is equal to 4 e+3 Pa.
- P_{exit} = -4812.76 Pa, and P_0 = 4 e+3 Pa.
- Base pressure Coefficient, $C_{Pe} = (p_4-p_0) / (½ *\rho*V_0^2)$,
- $\Delta P = (p4-p0) = (P_{exit} – P_0) = (-4812.76 -4000) = -8812.76$ Pa.
- Base pressure Coefficient, C_{P4} = -0.704.

Comparison of C_{Pe} of base diffuser with experimental results.

A=Ae/At	Cpe
For base diffuser, A= 5.098	**-0.704**
For NACA diffuser, A= 5.0	**-0.575**

- The Cpe values obtained for our Selig S1223 profile for the base diffuser was compared with the Cpe values obtained by Igra et. al. [2] for the NACA 4412 profile and a relative error of 22.4% was found.
- This can be mainly attributed to the increase in the negative pressure at the diffuser exit because of the Selg S1223 profile which shows better performance than NACA 4412 profile used by Igra.

Case 2: Analysis of static pressure at the exit of the 75 deg multi slot diffuser (x=0.0123m, y= 0m, z= 0 m)

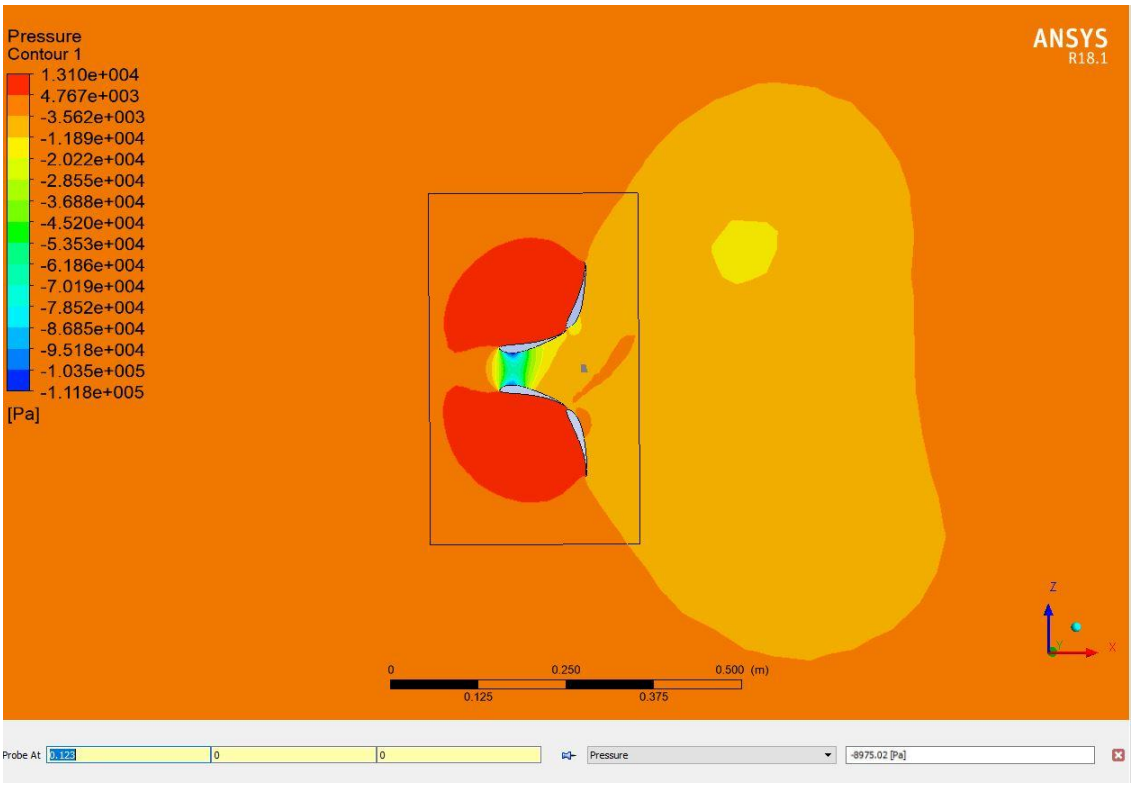

Fig 6.22. Probe at x=0.097m showing the pressure at the diffuser exit area

The static pressure at the diffuser exit is determined by using the probes at a distance of (x=0.123m, y= 0m, z= 0 m) and the value of P_{exit} is found to be equal to -4812.76 Pa.

- The inlet pressure at the entry of the diffuser P_0 is equal to 4 e+3 Pa
- P_{exit} = -8560.98 Pa, and P_0 = 4 e+3 Pa.
- Base pressure Coefficient, C_{P4} = (p4-p0) / (½ *ρ*V_0^2),
- ΔP= (p4-p0) = (Pexit – P0) = (-8975.02 -4000) =-12975. Pa.
- Base pressure Coefficient, C_{P4} = -1.038
- Thus, it is clearly evident that the 75 deg multi-lot diffuser has a strongly negative base pressure coefficient than that of the base diffuser.

CHAPTER 7: CONCLUSION

The performance of a multi slot diffuser for hydrokinetic energy conversion was investigated using ANSYS 18.1, for different angle of attacks of the secondary aerofoil and the comparison of the parameters was done with the base diffuser developed by A. Aranake [16]. The main conclusions are as follows:

- The 75^o multi-slot diffuser was found to have the maximum velocity at the throat, V_t = 17.45 m/s. with the velocity magnification factor of around 3.5. This can be attributed to the use of high lift aerofoil geometry Selig S1223, which increases the effective mass flow rate through the throat area.
- From the study of the pressure contours of the various orientations of the secondary diffuser, the 75^o multi-slot diffuser was found to have a very strong negative pressure at the exit of the diffuser P_{exit} = -8560.98 Pa, as compared to the base diffuser P_{exit} = -4812.76 Pa.
- Thus, from equation (2) mentioned above, Coefficient of power C_{Pi} can be directly linked to the Base pressure coefficient and as stated by Foreman et. al. [3], a strongly negative base pressure coefficient is highly favourable for the increase in the power coefficient of the turbine.

7.1. Future scope

Multi aerofoil diffusers are a promising field of research with the researchers diverging their attention towards this field.

- Experiments have been performed illustrating the use of flap rings etc, to enhance the performance of the diffuser.

- Experimental analysis of multi-slot diffusers utilizing these profiles can be done in the hydrodynamic test canal.

- K-epsilon turbulence model is used for solving this problem, better turbulence models can be used to enhance the results in future.
- However, further research can be done on studying the wake interactions of these multi-slot diffusers for possible array deployment.

REFERENCES

[1] G. M. Lilley, W.J. Rainbird, "preliminary report on the design and performance of ducted windmills," Department of Aerodynamics, Report no. 102, APRIL, 1956.

[2] Ozer Igra, "Compact shrouds for wind turbine," Energy Conversion, Vol. 16. Pp. 149-157, Pergamon Press, 1977.

[3] K. M. Foreman, B. gilbert and R. A. Oman, "Diffuser augmentation of wind turbines," Solar Energy, Vol. 20, pp. 305-31 I. Pergamon Press 1978.

[4] Fernando Ponta, Gautam Shankar Dutt, "An improved vertical-axis water-current turbine incorporating a channelling device," Renewable Energy 20, 2000,pp. 223-241.

[5] Toshiaki Setoguchi, Norimasa Shiomi, Kenji Kaneko, "Development of two-way diffuser for fluid energy conversion system," Renewable Energy 29, 2004,pp. 1757–1771.

[6] David L. F. Gaden and Eric L. Bibeau, "Increasing Power Density of Kinetic Turbines for Cost-effective Distributed Power Generation," Canada R3T 5V6.

[7] F.L. Pontaa, P.M. Jacovkis, "Marine-current power generation by diffuser-augmented floating hydro-turbines," Renewable Energy 33, 2008, pp. 665–673.

[8] M.J. Khan, G. Bhuyan, M.T. Iqbal, J.E. Quaicoe, "Hydrokinetic energy conversion systems and assessment of horizontal and vertical axis turbines for river and tidal applications: A technology status review," Applied Energy 86, 2009,pp. 1823–1835.

[9] David L.F. Gaden, Eric L. Bibeau, "A numerical investigation into the effect of diffusers on the performance of hydro kinetic turbines using a validated momentum source turbine model," Renewable Energy 35, 2010, pp. 1152–1158.

[10] Yuji Ohya and Takashi Karasudani, “A Shrouded Wind Turbine Generating High Output Power with Wind-lens Technology,” Energies 3, 2010, pp. 634–649.

[11] B.K. Kirke, “Tests on ducted and bare helical and straight blade Darrieus hydrokinetic turbines,” Renewable Energy 36, 2011, pp. 3013-3022.

[12] A.R. Malipeddi, D. Chatterjee, “Influence of duct geometry on the performance of Darrieus hydroturbine,” Renewable Energy 43, 2012, pp. 292-300.

[13]Philip C. Malte, James J. Riley, Igor V. Novosselov, “Analysis of Hydrokinetic Turbines in Open Channel Flows,” University of Washington, 2013.

[14] R. Luquet, D. Bellevre, D. Fréchou, P. Perdon, P. Guinard, “Design and model testing of an optimized ducted marine current turbine,” International journal of marine energy 2, 2013, pp. 61-80.

[15] E. Garcia, R. Piza, X. Benavides, E. Quiles, A. Correcher, and F. Morant, “Mechanical Augmentation Channel Design for Turbine Current Generators,”Advances in Mechanical Engineering, Volume 2014, Article ID 650131.

[16] Aniket C. Aranake, Vinod K. Lakshminarayan, Karthik Duraisamy, “Computational analysis of shrouded wind turbine configurations using a 3-dimensional RANS solver,” Renewable energy 75, 2015, pp. 815-832.

[17] Mohammad Shahsavarifard, Eric Louis Bibeau, Vijay Chatoorgoon, “Effect of shroud on the performance of horizontal axis hydrokinetic turbines,” Ocean engineering 96, 2015, pp. 215-225.

[18] N.W. Cresswell, G.L. Ingram, R.G. Dominy, “The impact of diffuser augmentation on a tidal stream turbine,” Ocean engineering 108, 2015, pp. 155-163.

[19] Jacob Riglin, Cosan Daskiran, Joseph Jonas, W. Chris Schleicher, Alparslan Oztekin a, “Hydrokinetic turbine array characteristics for river applications and spatially restricted flows,” Renewable energy 97, 2016, pp. 274-283.

[20] E. Chica, F. Perez, A. Rubio-Clemente, S. Agudelo, “Design of a hydrokinetic turbine,” Transactions on Ecology and The Environment, Vol 195, 2015.

[21] Uli Goltenbott, Yuji Ohya, Shigeo Yoshida, Peter Jamieson, “Aerodynamic interaction of diffuser augmented wind turbines in multi-rotor systems,” Renewable energy 112, 2017, pp. 25-34.

[22] Gonzalo Tampier, Claudio Troncoso, Federico Zilic, “Numerical analysis of a diffuser-augmented hydrokinetic turbine,” Ocean engineering 145, 2017, pp. 138-147.

[23] Muhammad Ilham Maulana, Ahmad Syuhada, Muhammad Nawawi2, “Analysis of Diffuser Augmented Wind Turbine (DAWT) with Flange and Curved Interior Using CFD,” International Conference on Thermal Science and Technology (ICTST), 2017.

[24] E. Chica, Edwar A. Torres, and J. Arbelaez, “Manufacture and experimental evaluation of a hydrokinetic turbine for remote communities in Colombia,” International Conference on Renewable Energies and Power Quality, 2018, ISSN 2172-038.

[25] “Inland waterways of India” Wikipedia, the free encyclopedia (https://en.wikipedia.org/wiki/Inland_waterways_of_India) , 2019.